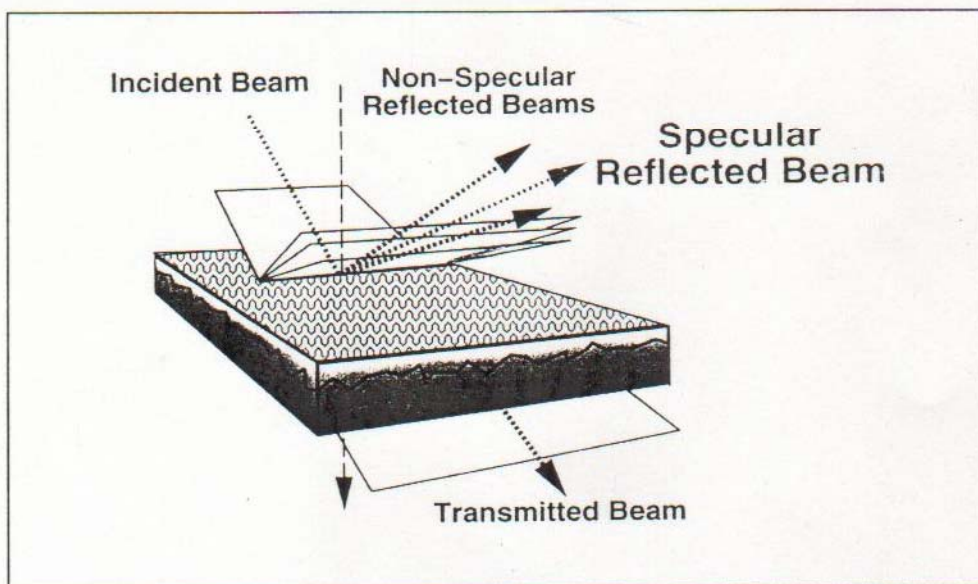


National School on Neutron and X-ray Scattering
August 15-29, 2004
Argonne National Laboratory



Fundamentals of X-Ray and Neutron Reflectometry



(Figure after
N.F. Berk)

C.F. Majkrzak

ICNR Researchers with a Major Interest in Reflectometry



R. Ivkov



S. Krueger



J. A. Borchers



J. A. Dura



S. K. Satija



M. Tarek



N. F. Berk



K. T. Forstner



A. Schreyer



C. F. Majkrzak

K. O'Donovan U. Perez-Salas M. Wang L. Kneller
Young Soo Seo

PROBES OF THE MICROSTRUCTURE OF SURFACES AND INTERFACES

photons, electrons, neutrons, atom and ion beams, miniature mechanical devices

* DIRECT IMAGING (REAL SPACE)

e.g.:

- optical microscopy (~ 1000 x magnification)
- scanning electron microscopy (SEM) (orders of magnitude higher magnification than possible with light)
- transmission electron microscopy (TEM)
- atomic force microscopy (AFM)

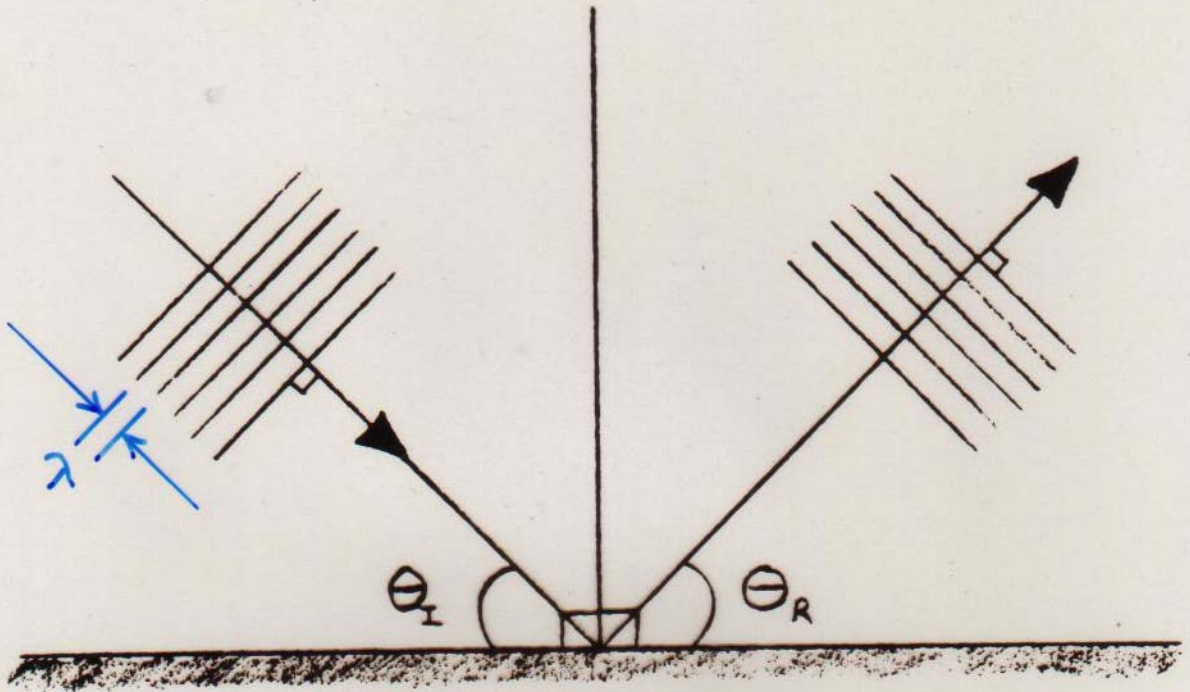
* DIFFRACTION (RECIPROCAL SPACE)

e.g.:

- low energy electron diffraction (LEED)
- spin polarized LEED (SPLEED)
- reflection high energy electron diffraction (RHEED)
- ellipsometry (optical polarimetry)
- x-ray reflectometry
- neutron reflectometry

For quantitative measurements of depth profiles along a normal to the surface, x-ray and neutron reflectometry are particularly useful because of their relatively weak interactions with condensed matter and the fact that these interactions can be described accurately by a comparatively simple theory. In the case of electron diffraction, on the other hand, the potential is non-local and the scattering is non-spherical, relatively strong and highly energy-dependent. For atom diffraction, the description of the interaction potential can be even more complicated.

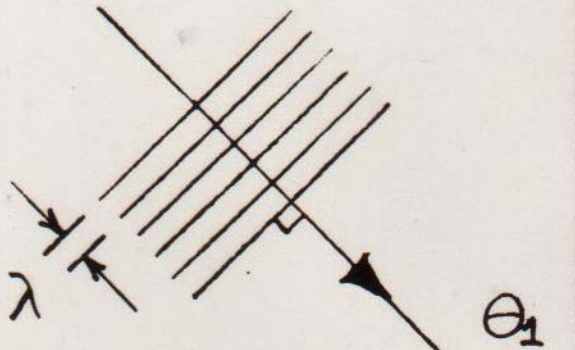
"SPECULAR" OR "MIRROR" REFLECTION
OF A WAVE



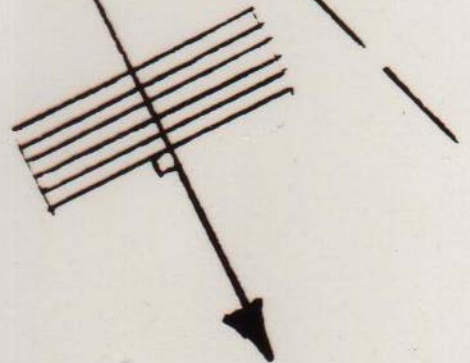
ANGLE OF INCIDENCE θ_i
= ANGLE OF REFLECTION θ_r

$n_1 = 1$
(FOR VACUUM)

$$n_1 \sin \theta_1 = n_2 \sin \theta_2$$



θ_2



$n_2 = 1.581$
(CERTAIN GLASS)

WAVE SPEED $C = \frac{C_0 \text{ (VACUUM)}}{n}$

WAVE-LENGTH $\lambda = \frac{\lambda_0}{n}$

WAVE-VECTOR $k = nk_0 = \frac{2\pi\nu}{c}$

FREQUENCY $\nu = \text{CONSTANT}$

REFRACTIVE INDEX n DEPENDS ON MATERIAL AND WAVELENGTH OF THE LIGHT

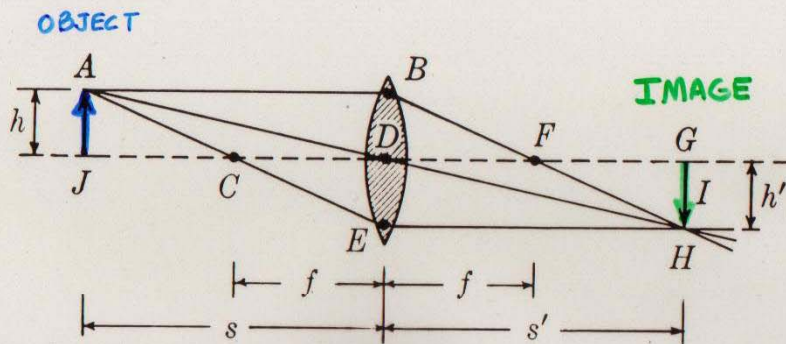


Figure 44-10. Geometrical relations among object distance s , image distance s' , and focal length f .

(from Weidner & Sells, *Elementary Classical Physics*)

$$\frac{1}{f} = \frac{1}{s} + \frac{1}{s'}$$

$$\frac{h}{s} = \frac{h'}{s'}$$

The ratio of image-object distances, s'/s , is equal to the ratio of in object sizes, h'/h . This ratio h'/h is known as the *lateral magnification*.

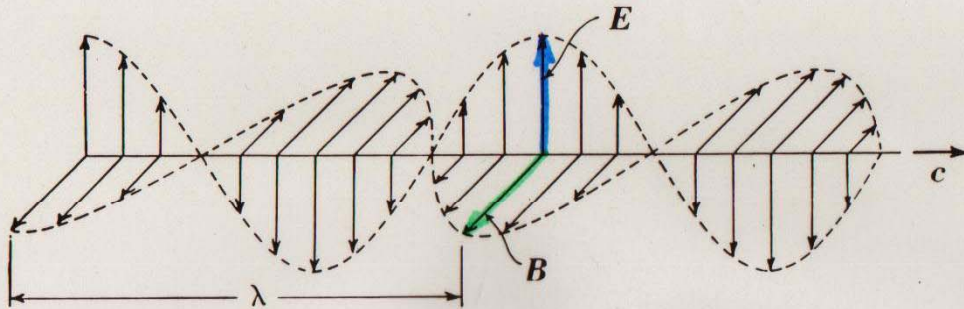
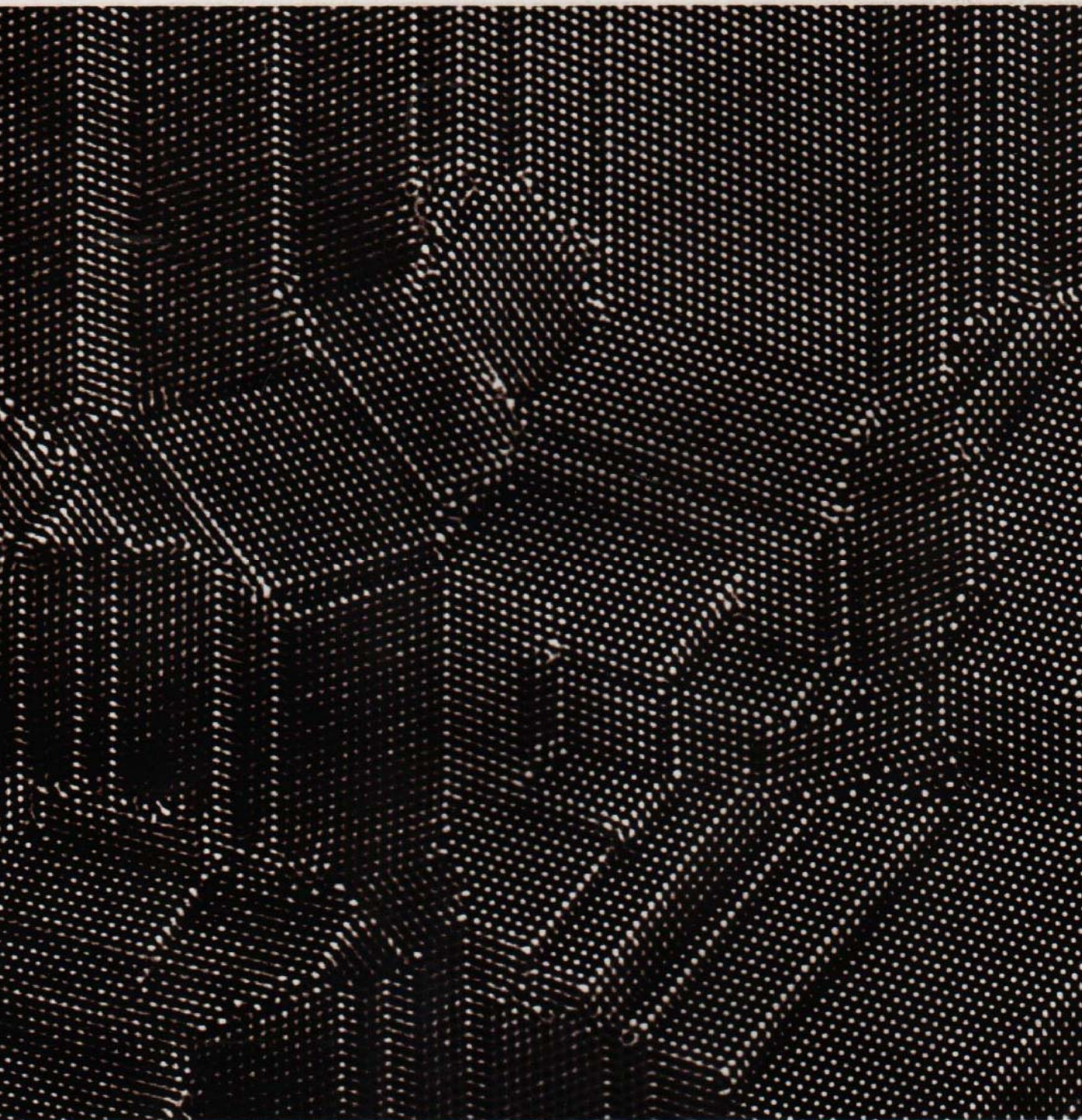


Figure 41-15. Representations of the electric and magnetic fields of a sinusoidal electromagnetic wave: (a) the field lines; (b) the sinusoidally varying amplitudes. (after Weidner & Sells, Elementary Classical Physics)

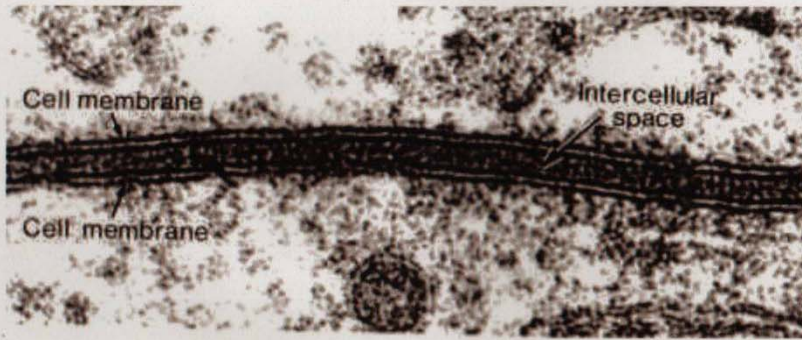
PHOTON

- ZERO MASS
- VELOCITY (IN VACUUM)
 $c_0 \approx 3 \times 10^8 \text{ m/sec}$
- POLARIZED ELECTROMAGNETIC WAVE



Atomic resolution micrograph of multiply-twinned nanocrystalline film of Si. (C. Song)

(LAWRENCE-BERKELEY LAB.)



(AFTER BLOOM & FANGETT, A TEXTBOOK OF HISTOLOGY)

(from Photonics
by Saleh & Teich)

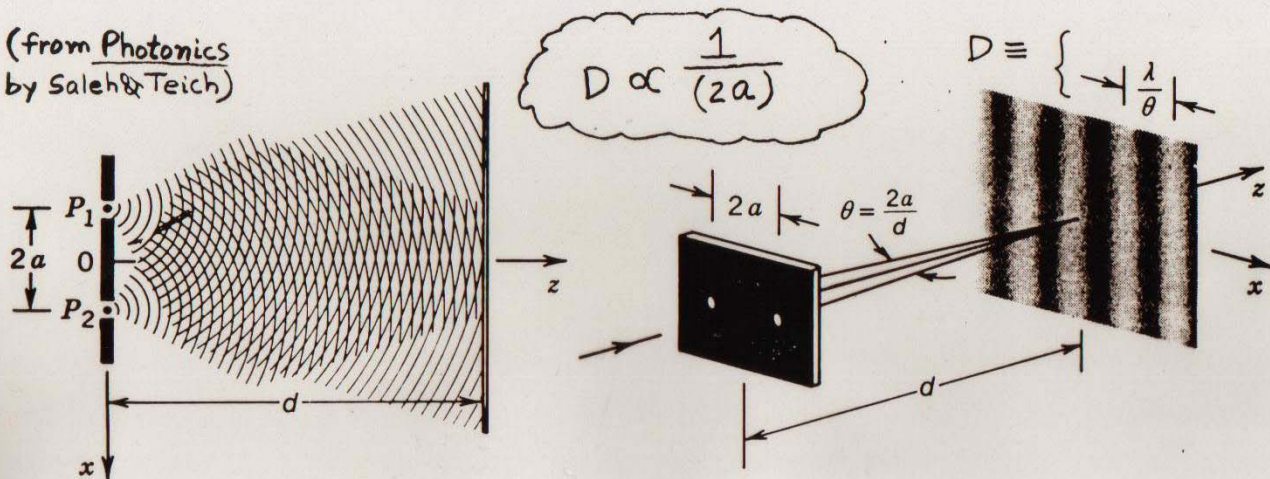
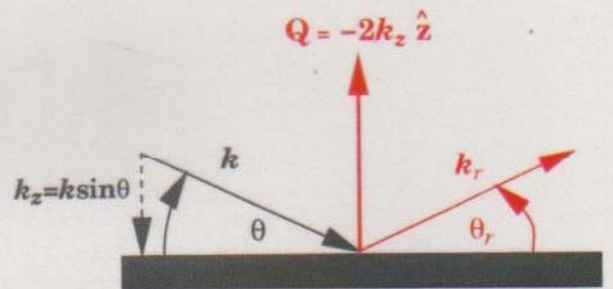
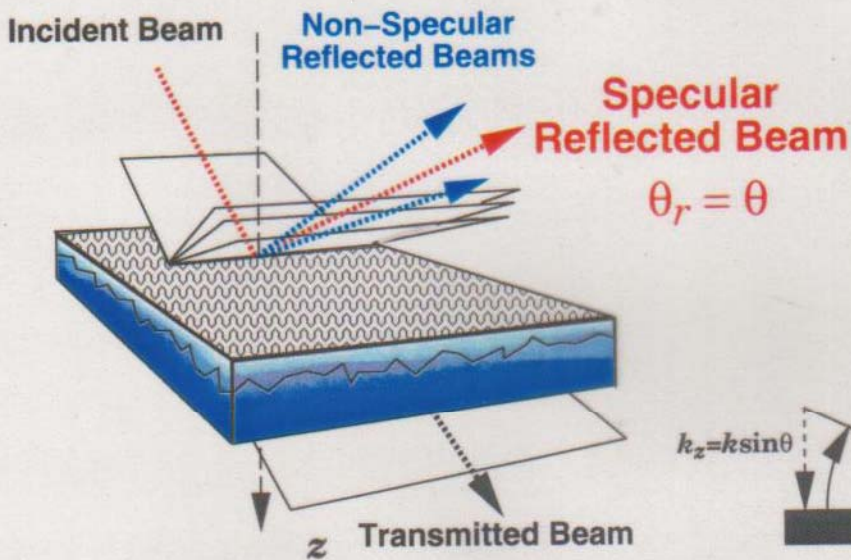


Figure 2.5-6 Interference of two spherical waves of equal intensities originating at the points P_1 and P_2 . The two waves can be obtained by permitting a plane wave to impinge on two pinholes in a screen. The light intensity at an observation plane a distance d away takes the form of a sinusoidal pattern with period $\approx \lambda/\theta$.

DIFFRACTION PATTERN WHICH RESULTS FROM THE COHERENT SUPERPOSITION OF TWO WAVES (AMPLITUDES OF THE TWO WAVES ADD TOGETHER AT ANY GIVEN POINT IN SPACE)

A CHARACTERISTIC RECIPROCAL RELATIONSHIP EXISTS BETWEEN THE POSITIONS OF THE INTENSITY MAXIMA IN THE DIFFRACTION PATTERN AND THE DISTANCE SEPARATING THE OBJECTS CAUSING THE SCATTERING.

$$\text{Reflectivity} = \frac{\text{Number of reflected neutrons}}{\text{Number of incident neutrons}} = |r|^2$$



Specular reflection: $\bar{\rho}(z) = \langle \rho(x, y, z) \rangle_{xy}$

Non-Specular reflection: $\Delta\rho(x, y, z) = \rho(x, y, z) - \bar{\rho}(z)$

(AFTER N.F. BERK ET AL.)

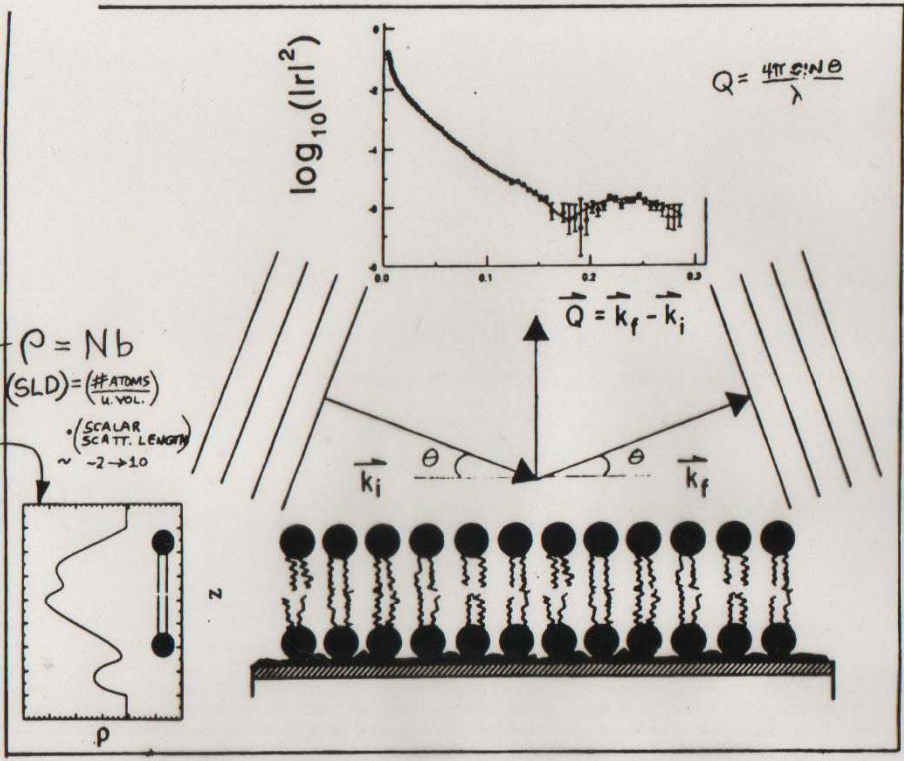


Fig. 1

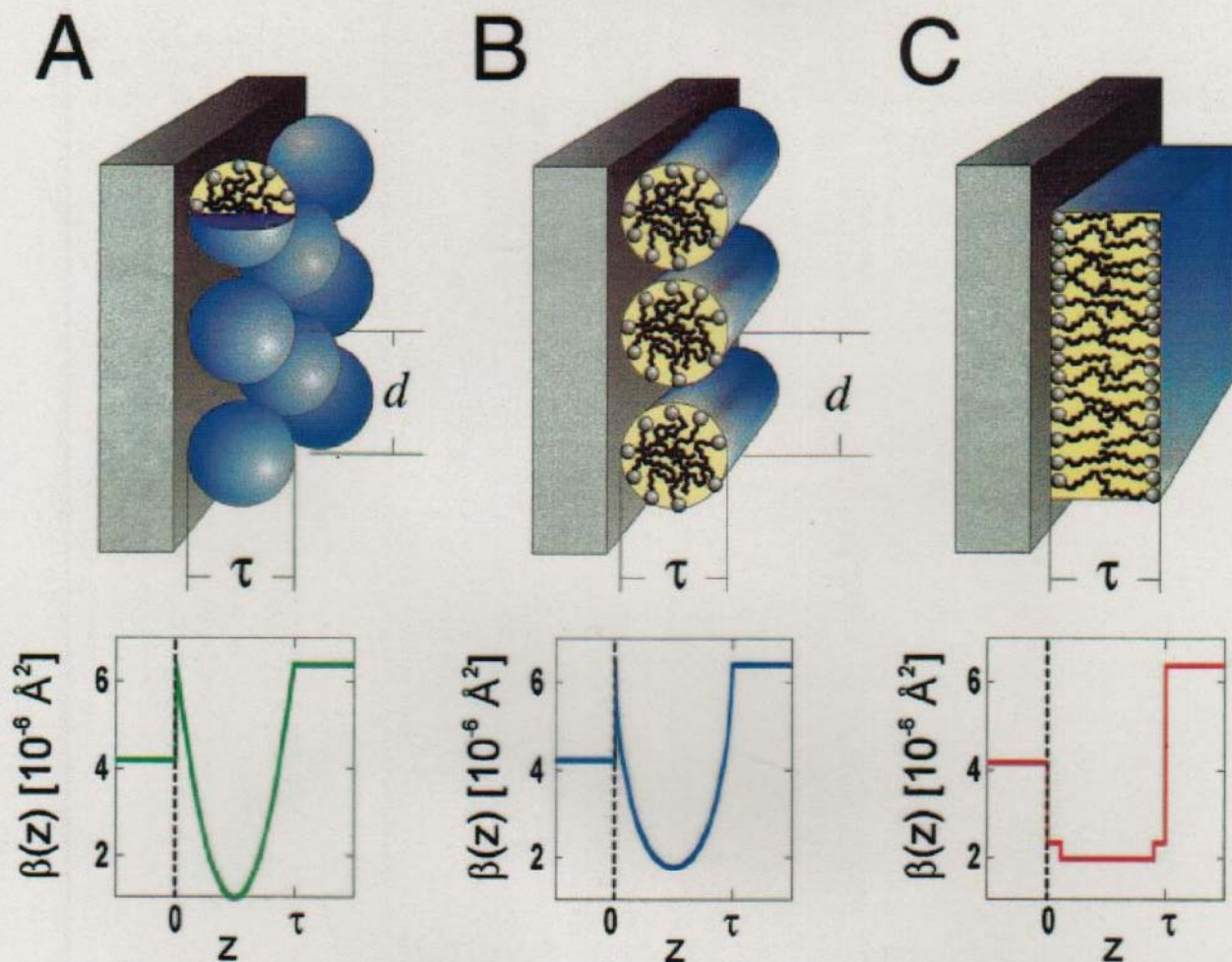


FIG. 1. (Color) Schematic diagram of adsorbed layer structures consisting of (A) spherical micelles, (B) cylindrical micelles, and (C) a bilayer, including the film thickness τ and interaggregate spacing d . Also shown are examples of neutron scattering length density profiles normal to the interface, $\beta(z)$, corresponding to each structure at the quartz/D₂O interface at a fractional surface coverage of 0.55. The head-group and alkyl tails of the surfactants have different scattering length densities, but because of the arrangement of the molecules this is only apparent in the bilayer $\beta(z)$.

single-crystal quartz block and reflected from the quartz-solution interface were recorded as a function of angle of incidence. The off-specular background, including any signal due to scattering from the bulk solution [15], was subtracted to give the reflection coefficient of the surfactant-coated interface. All solutions used were above their critical micelle

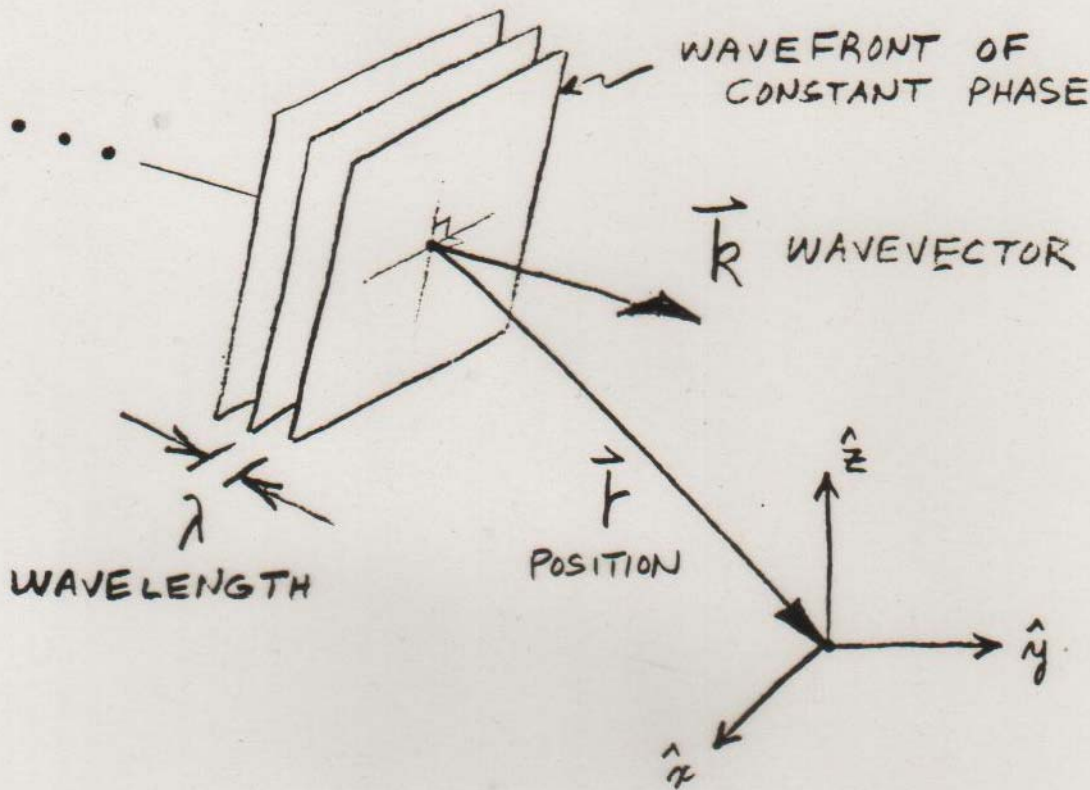
or aggregation concentration, a condition which leads to a saturated adsorbed film at the solid-solution interface.

The cationic surfactant tetradecyltrimethylammonium bromide (TTAB) forms nearly spherical micellar aggregates consisting of approximately 80 molecules in bulk solution. Small angle neutron-scattering measurements [16] give mi-



FIG. 2. 200 \times 200-nm² AFM tip deflection images of (A) spherical TTAB aggregates adsorbed onto quartz from water solution, (B) cylindrical TTAB aggregates adsorbed onto quartz from an aqueous 200mM NaBr solution, and (C) planar DDAB bilayer adsorbed onto quartz from water solution. Long-wavelength undulations visible in (B) and (C) arise from roughness in the underlying quartz.

WAVE PROPAGATING IN FREE SPACE



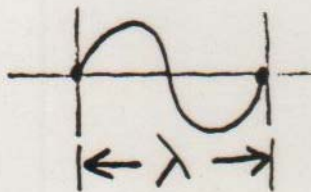
WAVEFUNCTION

$$\Psi \propto e^{i \vec{k}_0 \cdot \vec{r}}$$

$$\begin{cases} \vec{k}_0 = k_{0x} \hat{x} + k_{0y} \hat{y} + k_{0z} \hat{z} \\ \vec{r} = x \hat{x} + y \hat{y} + z \hat{z} \end{cases}$$

FOR \vec{k}_0 ALONG \hat{z} , FOR EXAMPLE,

$$\Psi \propto \cos(k_{0z} z) + i \sin(k_{0z} z)$$



$$\left(\frac{2\pi}{\lambda} z \right)$$

$|\Psi|^2 \propto$ PROBABILITY OF THE NEUTRON BEING THERE

FOR ELASTIC INTERACTIONS
TOTAL ENERGY OF THE
NEUTRON IS CONSTANT

$$\begin{aligned}\text{TOTAL ENERGY} &= \text{KINETIC ENERGY} \\ &+ \text{POTENTIAL ENERGY} \\ &= \text{CONSTANT}\end{aligned}$$

WAVE EQUATION OF MOTION
(SCHRÖDINGER EQUATION)

$$\underbrace{\left[\frac{-\hbar^2}{2m} \nabla^2 \right]}_{\text{K.E.}} + \underbrace{V(\vec{r})}_{\text{P.E.}} \underbrace{\Psi}_{\text{T.E.}} = E \Psi$$

$$\nabla^2 = \frac{\partial^2}{\partial x^2} + \frac{\partial^2}{\partial y^2} + \frac{\partial^2}{\partial z^2}$$

IN VACUUM

$$\text{K.E.}_0 = \frac{\hbar^2 k_0^2}{2m}$$

$$V(\vec{r}) = \frac{2\pi\hbar^2}{m} \sum_{j=1} N_j b_j = \frac{2\pi\hbar^2}{m} \rho$$

$$b = \text{Re}b + i\text{Im}b$$

NUMBER OF ATOMS OF TYPE j PER UNIT VOLUME \nearrow
 COHERENT SCATTERING "LENGTH" OF ATOM j \nwarrow

ρ = "SCATTERING LENGTH DENSITY" (SLD)

IN VACUUM:

$$E_0 = \frac{\hbar^2 k_0^2}{2m} + 0$$

IN A MATERIAL MEDIUM:

$$E = \frac{\hbar^2 k^2}{2m} + \frac{2\pi\hbar^2}{m} \rho$$

CONSERVATION OF ENERGY
REQUIRES $E_0 = E$

$$\therefore k^2 = k_0^2 - 4\pi\rho$$

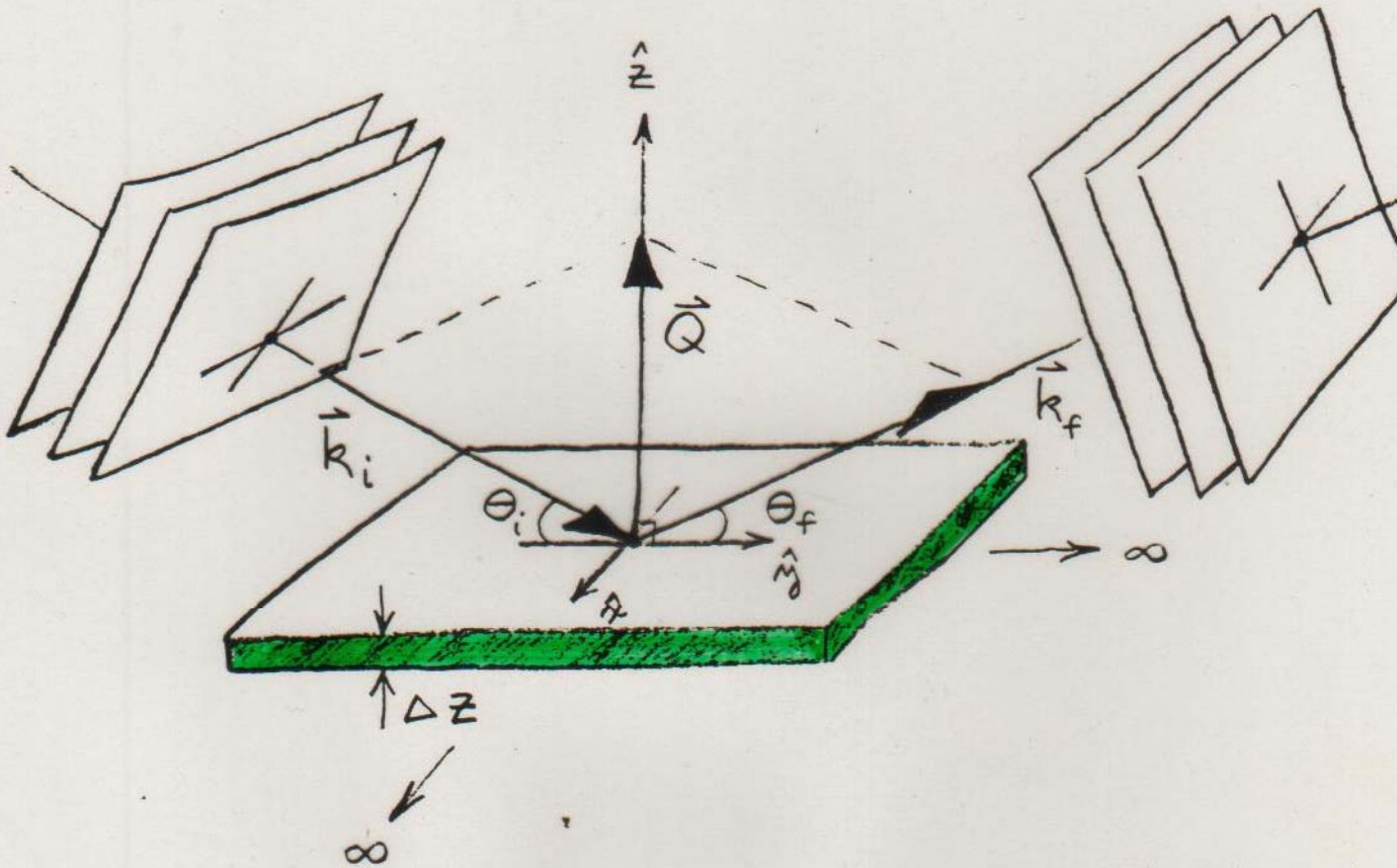
THUS

$$[\nabla^2 + k^2] \Psi = 0$$

NOTE REFRACTIVE INDEX $n \equiv \frac{k}{k_0}$:

$$n^2 = 1 - \frac{4\pi\rho}{k_0^2}$$

REFLECTION FROM AN IDEAL FILM OR SLAB OF MATERIAL



WAVEVECTOR TRANSFER $\vec{Q} = \vec{k}_f - \vec{k}_i$

$\rho = \rho(z)$ ONLY

EXPANDING $k^2 = k_0^2 - 4\pi\rho$,

$$k_x^2 + k_y^2 + k_z^2 + 4\pi\rho = k_{0x}^2 + k_{0y}^2 + k_{0z}^2.$$

NOW IF $\rho = \rho(z)$ ONLY, THEN

$$\frac{\partial \rho}{\partial x} \text{ AND } \frac{\partial \rho}{\partial y}, \text{ WHICH ARE}$$

PROPORTIONAL TO THE GRADIENTS OF THE POTENTIAL OR FORCES IN THE RESPECTIVE DIRECTIONS, ARE EQUAL TO ZERO. THUS, NO FORCE ACTS ALONG THESE DIRECTIONS TO CHANGE k_x AND k_y . THEN

$$k_x = k_{0x} \text{ AND } k_y = k_{0y} \text{ ARE}$$

"CONSTANTS OF THE MOTION".

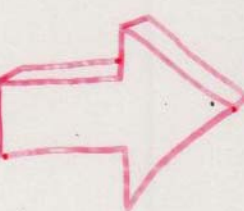
SUBSTITUTING $\underline{\Psi}(\vec{r}) = e^{ik_{0x}x} e^{ik_{0y}y} \underline{\Psi}(z)$

INTO $[\nabla^2 + k^2] \underline{\Psi} = 0$ GIVES

$$\left[\frac{\partial^2}{\partial z^2} + k_z^2 \right] \underline{\Psi}(z) = 0$$

BECAUSE THERE IS NO CHANGE IN THE POTENTIAL IN THE X- OR Y- DIRECTIONS, THERE CAN BE NO MOMENTUM CHANGE IN THESE DIRECTIONS EITHER

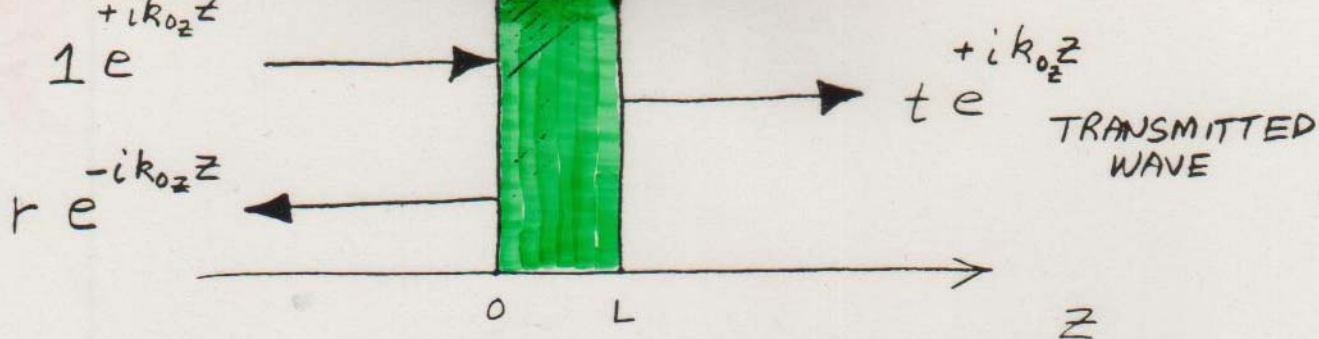
THE IDEAL SLAB GEOMETRY WITH $\rho = \rho(z)$ ONLY GIVES RISE TO THE COHERENT "SPECULAR" REFLECTION OF A PLANE WAVE WHICH IS DESCRIBED BY A ONE-DIMENSIONAL WAVE EQUATION:


$$\left[\frac{\partial^2}{\partial z^2} + k_{0z}^2 - 4\pi\rho(z) \right] \psi(z) = 0$$

IN THIS CASE $\theta_i = \theta_f \equiv \theta$,

$$|\vec{k}_i| = |\vec{k}_f| \quad \text{AND} \quad Q = 2k \sin \theta \\ = 2k_z$$

ALSO, $n_z^2 \equiv 1 - \frac{4\pi\rho(z)}{k_{0z}^2}$



$$Q = z k_{0z}$$

FROM THE WAVE EQUATION,
IT IS POSSIBLE TO FIND
A SOLUTION FOR THE
REFLECTION AMPLITUDE IN
INTEGRAL FORM
(SEE ARTICLE PAGES) :

$$r(Q) = \frac{4\pi}{iQ} \int_{-\infty}^{+\infty} \psi(z) \rho(z) e^{+ik_0 z z} dz$$

WHAT IS LOCALIZED AT z IN
THE SLD PROFILE $\rho(z)$ IN
"REAL" SPACE, IS DISTRIBUTED
OVER THE REFLECTION AMPLITUDE
 $r(Q)$ IN THE RELATED SCATTERING
OR "RECIPROCAL" SPACE

$\psi(z)$ INSIDE THE MEDIUM
IS GENERALLY UNKNOWN:

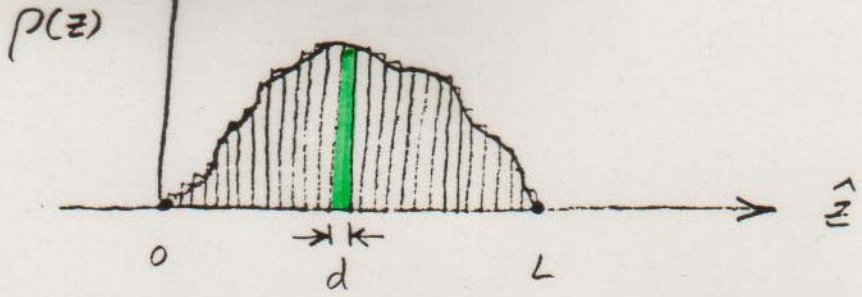
BORN APPROXIMATION REPLACES
 $\psi(z)$ WITH THE INCIDENT
WAVE FUNCTION e^{+ik_0z} BASED
ON THE ASSUMPTION THAT
 $\psi(z)$ IS NOT SIGNIFICANTLY
DISTORTED FROM THE FREE
SPACE FORM (WEAK
INTERACTION): THEN

$$r(Q) \approx \frac{4\pi}{iQ} \int_{-\infty}^{+\infty} p(z) e^{iQz} dz$$

FOURIER
TRANSFO

FOR A REAL POTENTIAL $p(z)$

$$\text{Re } r(Q) \approx \frac{4\pi}{Q} \int_{-\infty}^{+\infty} p(z) \sin(Qz) dz$$



ARBITRARY POTENTIAL DIVIDED INTO
RECTANGULAR SLABS OF WIDTH
d AND CONSTANT ρ

THEN

(BORN APPROX)

$$\text{Re } r(Q) \approx \frac{4\pi}{Q} \int_0^L p(z) \sin(Qz) dz$$

BECOMES

$$\begin{aligned} \text{Re } r(Q_j) &\approx \frac{4\pi}{Q_j} \sum_{l=1}^N \int_{(l-1)d}^{ld} \rho_l \sin(Q_j z) dz \\ &= -\frac{4\pi}{Q_j^2} \sum_{l=1}^N \rho_l \left[\cos(Q_j z) \right]_{(l-1)d}^{ld} \end{aligned}$$

SET OF
EQUATIONS FOR
DIFFERENT
VALUES OF
OR θ

$$\left\{ \begin{aligned} \text{Re } r_1 &= \zeta_{11} P_1 + \zeta_{12} P_2 + \dots + \zeta_{1N} P_N \\ \text{Re } r_2 &= \zeta_{21} P_1 + \zeta_{22} P_2 + \dots + \zeta_{2N} P_N \\ &\vdots \\ \text{Re } r_N &= \zeta_{N1} P_1 + \zeta_{N2} P_2 + \dots + \zeta_{NN} P_N \end{aligned} \right.$$

SOLVE SIMULTANEOUS EQUATIONS FOR P_i 's GIVEN $\text{Re } r_i$'s
e.g., SVD, EIGENVALUE PROBLEM FORMULATION, ...

$$\underbrace{\operatorname{Re} r_{BA}(Q) \left[\frac{Q^2}{8\pi \sin\left(\frac{Qd}{2}\right)} \right]}_{\equiv \mathcal{I}(Q)} = \sum_{j=1}^N \rho_j \sin\left[\frac{(2j-1)Qd}{2} \right]$$

$$\int_0^{\pi} \sin m\theta \sin n\theta d\theta = \begin{cases} 0 & m, n \text{ INTEGERS, } m \neq n \\ \frac{\pi}{2} & m, n \text{ INTEGERS, } m = n \end{cases}$$

ORTHOGONALITY

$$\rho_j = \frac{d}{4\pi^2} \int_0^{\frac{\pi}{d}} Q^2 \operatorname{Re} r_{BA}(Q) \frac{\sin\left[\frac{(2j-1)Qd}{2}\right]}{\sin\left(\frac{Qd}{2}\right)} dQ$$

$$2\theta = 180$$

$$\left(= \frac{4\pi}{\lambda} \sin(90^\circ) \right)$$

$\lambda(\text{\AA})$

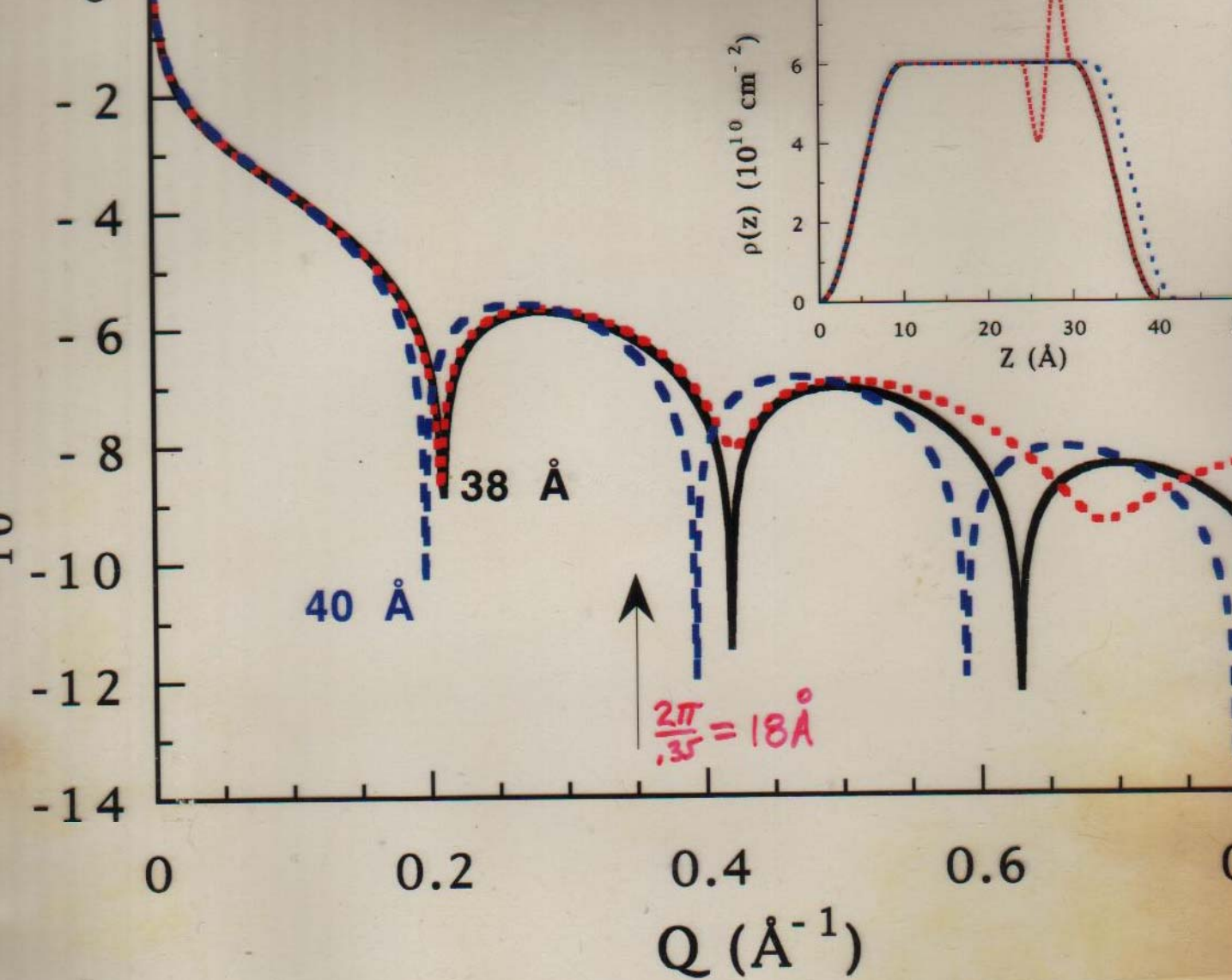
$Q_{\text{MAX}} (\text{\AA}^{-1})$

$$D_{\text{MIN}}(\text{\AA}) = \frac{2\pi}{Q_{\text{MAX}}} = \frac{\lambda}{2}$$

5
10
50
100
500
1000
5000

2.513
1.256
0.251
0.125
0.025
0.012
0.002

2.5
5
25
50
250
500
2500



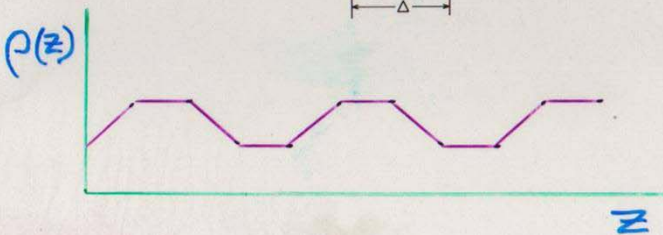
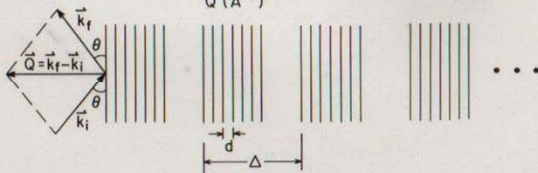
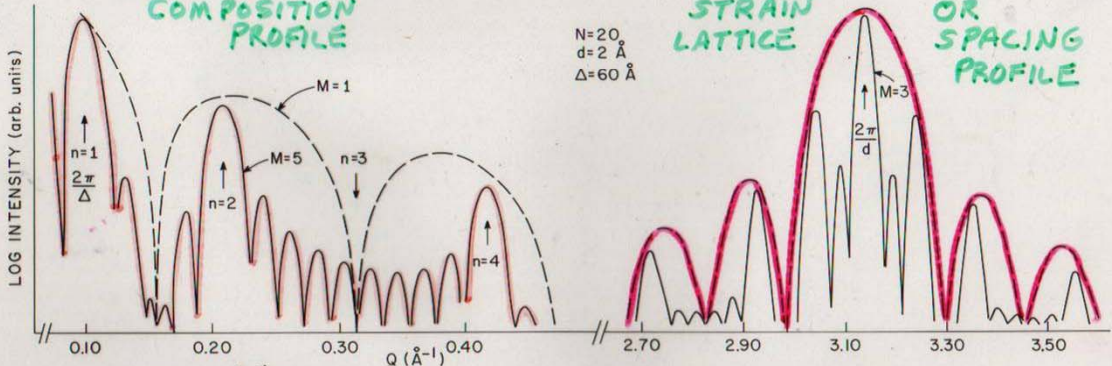
Solid, long-dash, and short-dash neutron reflectivity curves corresponding to their respective scattering length density profiles shown in the inset. This series of curves and profiles illustrates the sensitivity of the reflectivity to the overall film thickness at reflectivities approaching 10^{-7} whereas detailed features such as the oscillation in the long-dash profile can only be accurately discerned at reflectivities an order of magnitude or so lower, at Q -values corresponding to $2\pi/\text{width of the feature}$.

"REFLECTIVITY" REGIME

"DIFFRACTION" REGIME

LOW Q : HIGHER SENSITIVITY FOR COMPOSITION PROFILE

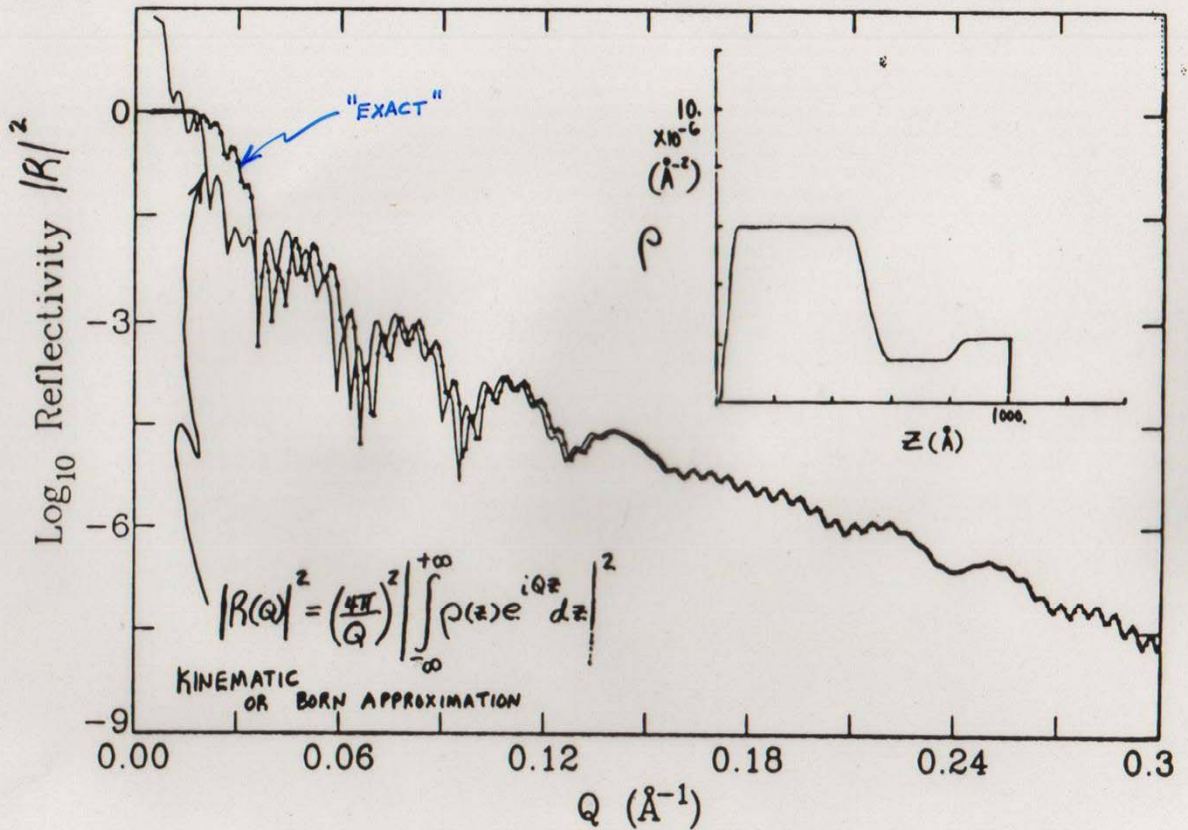
HIGH Q : HIGHER SENSITIVITY FOR STRAIN LATTICE OR SPACING PROFILE



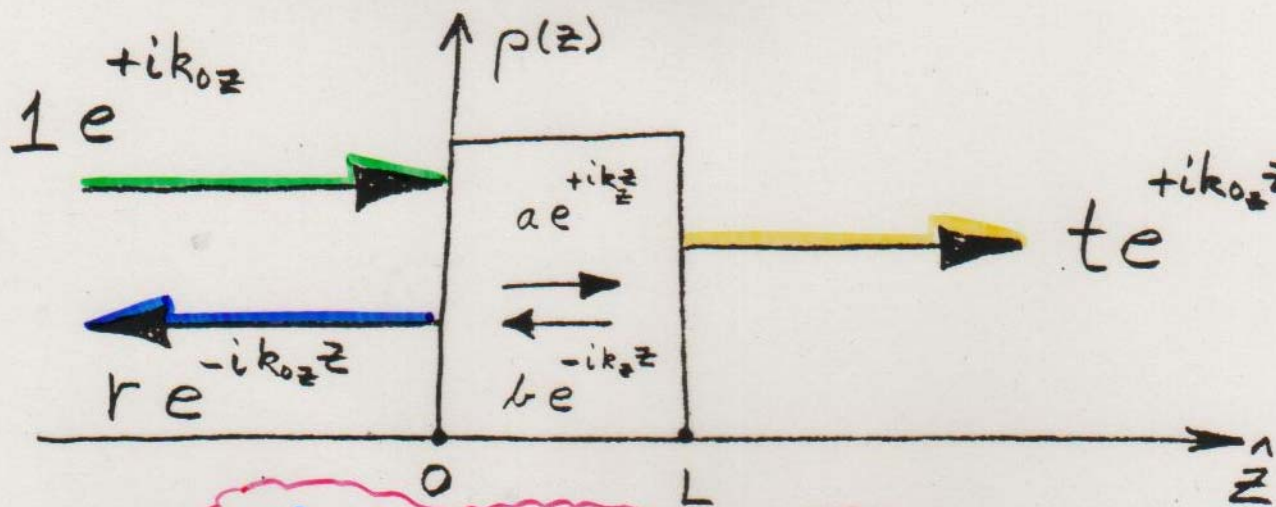
$$|R|_{KIN}^2 = \left(\frac{4\pi}{Q} \right)^2 \left| \sum_{m=1}^M \sum_{n=1}^N \rho e^{iQ(md+n\Delta)} \right|^2$$

$$= \left(\frac{4\pi}{Q} \right)^2 \rho^2 \left| \frac{\sin(NQd/2)}{\sin(Qd/2)} \right|^2 \left| \frac{\sin(MQ\Delta/2)}{\sin(Q\Delta/2)} \right|^2$$

PROBLEM: BORN APPROXIMATION FAILS AT SUFFICIENTLY SMALL Q — MUST THEN USE EXACT THEORY



Comparison between kinematic (line) and dynamic (triangle + line) plus-state reflectivities for a density profile similar to that of Fig.2 as described in the text.



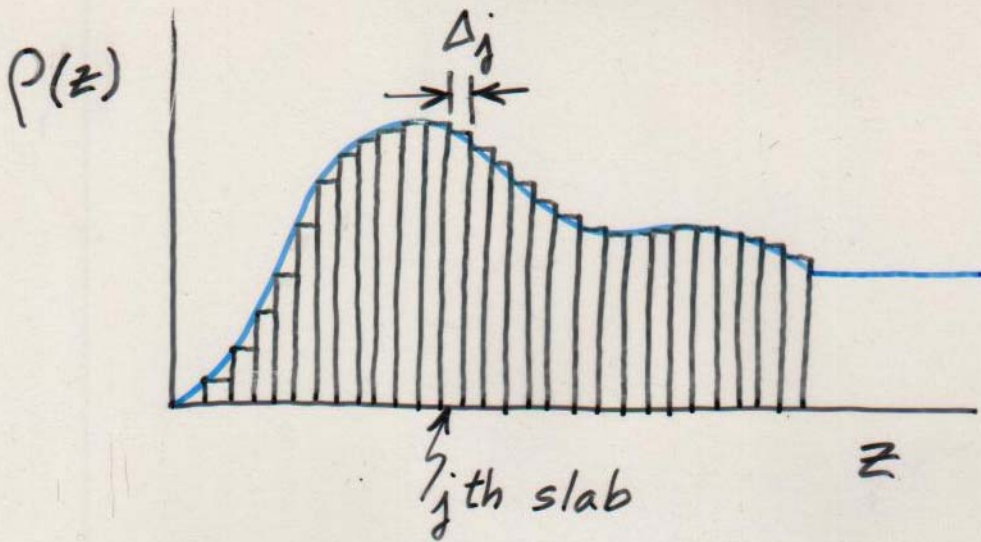
$$\frac{\partial^2 \psi(z)}{\partial z^2} + k_z^2 \psi(z) = 0$$

CONSERVATION OF MOMENTUM
AND PARTICLE NUMBER

REQUIRE THAT $\frac{\partial \psi(z)}{\partial z}$ AND $\psi(z)$

BE CONTINUOUS AT THE
BOUNDARIES $z=0$ & $z=L$

$$\begin{pmatrix} t \\ it \end{pmatrix} e^{ik_0z L} = \begin{pmatrix} A & B \\ C & D \end{pmatrix} \begin{pmatrix} 1+r \\ i(1-r) \end{pmatrix}$$



$$\begin{pmatrix} A & B \\ C & D \end{pmatrix} = \begin{pmatrix} a_N & b_N \\ c_N & d_N \end{pmatrix} \begin{pmatrix} a_{N-1} & b_{N-1} \\ c_{N-1} & d_{N-1} \end{pmatrix} \cdots \begin{pmatrix} a_2 & b_2 \\ c_2 & d_2 \end{pmatrix} \begin{pmatrix} a_1 & b_1 \\ c_1 & d_1 \end{pmatrix}$$

$$\begin{pmatrix} a_j & b_j \\ c_j & d_j \end{pmatrix} = \begin{pmatrix} \cos S_j & \frac{1}{m_{zj}} \sin S_j \\ -m_{zj} \sin S_j & \cos S_j \end{pmatrix}$$

$$\begin{aligned} S_j &= k_{0z} m_{zj} \Delta_j \\ &= k_{zj} \Delta_j \end{aligned}$$

free film

Then, once we know $M_k(L)$:

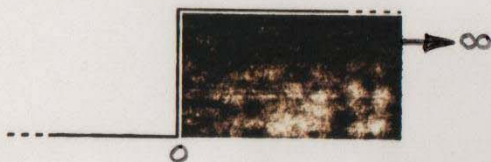
$$\begin{array}{ccc} \boxed{z=L} & & \boxed{z=0} \\ \left(\begin{array}{c} 1 \\ i \end{array} \right) t(k) e^{ikL} & = & \begin{pmatrix} A_k(L) & B_k(L) \\ C_k(L) & D_k(L) \end{pmatrix} \begin{pmatrix} 1+r(k) \\ i[1-r(k)] \end{pmatrix} \end{array}$$

$$r = \frac{B+C + i(D-A)}{B-C + i(D+A)}$$

$$t = \frac{2ie^{-ikL}}{B-C + i(D+A)}$$

$$R = |r|^2 = \frac{\Sigma-2}{\Sigma+2}, \quad \Sigma = A^2 + B^2 + C^2 + D^2$$

Fresnel Reflectivity

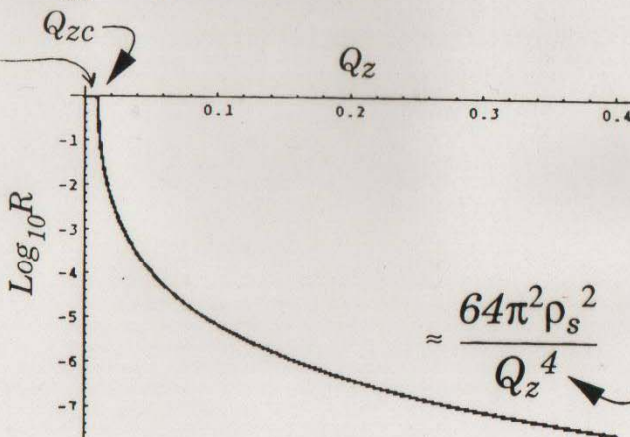


$$|r_F|^2 \equiv R_F(Q_z)$$

$$R_F(Q_z) = \frac{1 - \sqrt{1 - \frac{Q_{zc}^2}{Q^2}}}{1 + \sqrt{1 - \frac{Q_{zc}^2}{Q^2}}}$$

For $Q_z < Q_{zc}$, $R_F = 1$.

MIRROR
REFLECTION
PLATEAU



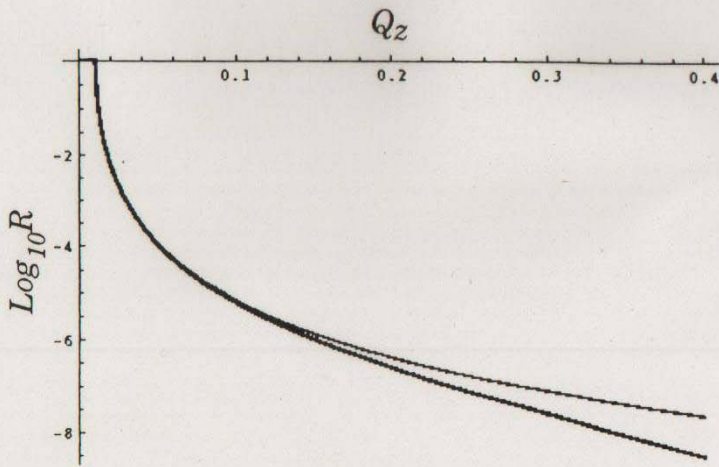
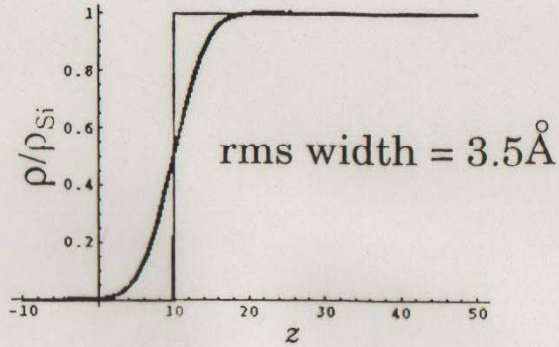
"CRITICAL
Q"

$$Q_c^2 = 16\pi\rho$$

(N.F. BERK)

"Soft" substrate

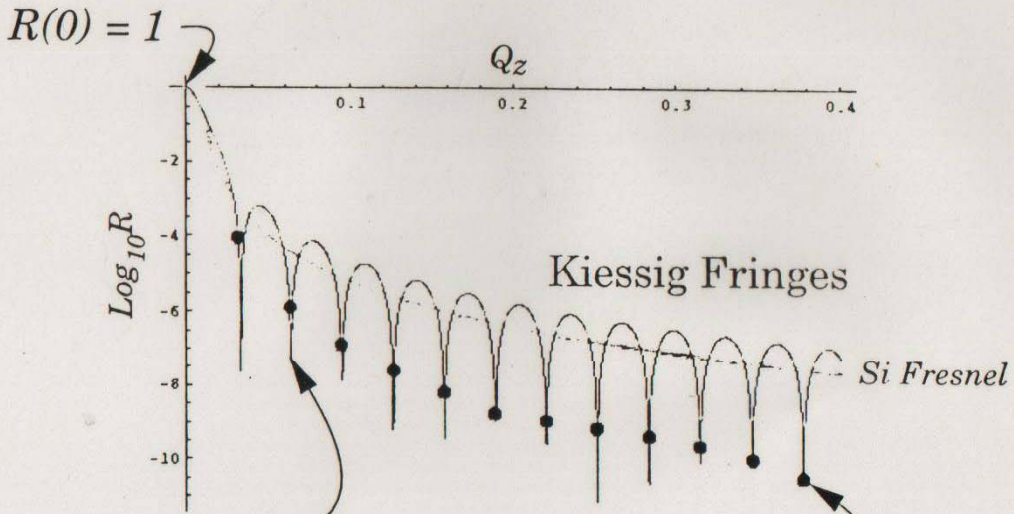
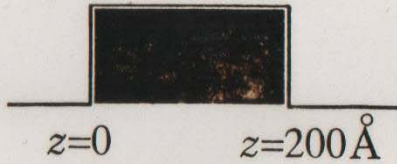
Smooth transition:
interlayer diffusion
roughness



(N.F. BERK)

Uniform slab

$$\rho = 2.07 \cdot 10^{-6} \text{ \AA}^{-2}$$



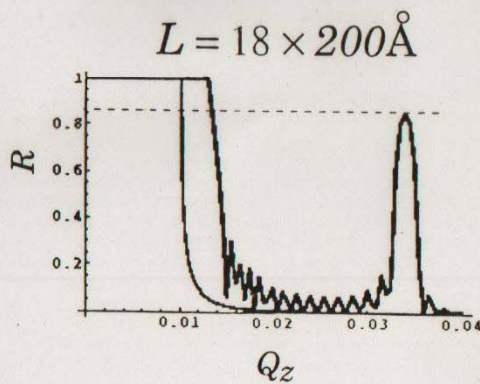
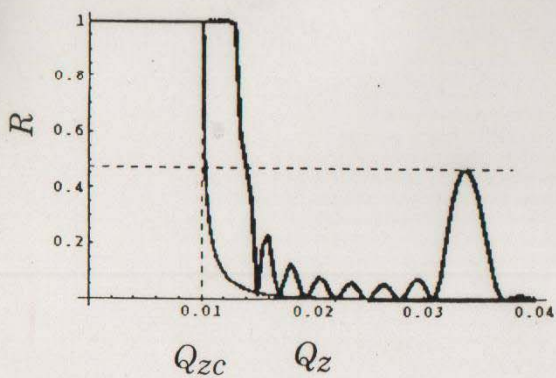
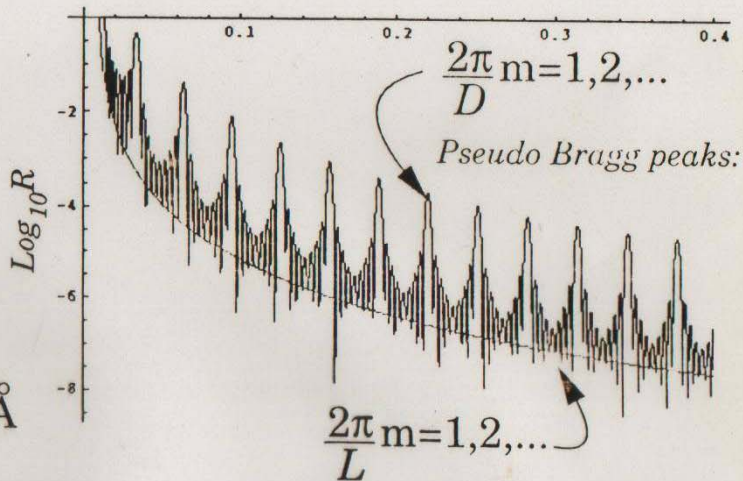
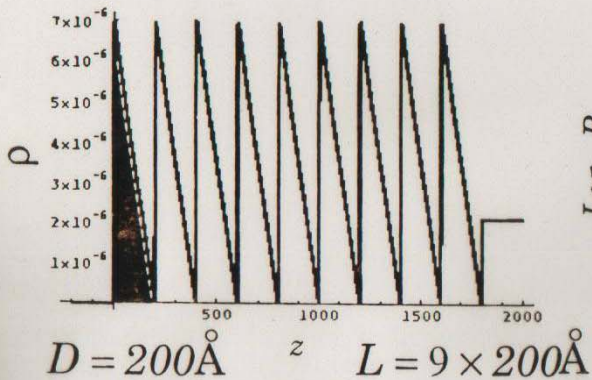
$$\sqrt{Q_z^2 - 16\pi\rho} = \frac{2\pi}{L} m = 1, 2, \dots$$

$$\frac{2\pi}{L} m = 1, 2, \dots$$

(Kinematical)

(N.F. BERK)

Multilayer on Si



(N.F. BERK)

IF ρ IS NOT EXACTLY $\rho(z)$,
 I.E., SOME VARIATIONS EXIST IN
 THE (x, y) - PLANE, THEN

ON SPECULAR
 "RIDGE"
 WHERE $\vec{Q} = Q_z \hat{z}$

$$r_{\text{BORN}} \approx \frac{4\pi}{iQ} \int_{-\infty}^{+\infty} \langle \rho(x, y, z) \rangle_{x, y} e^{iQz} dz$$

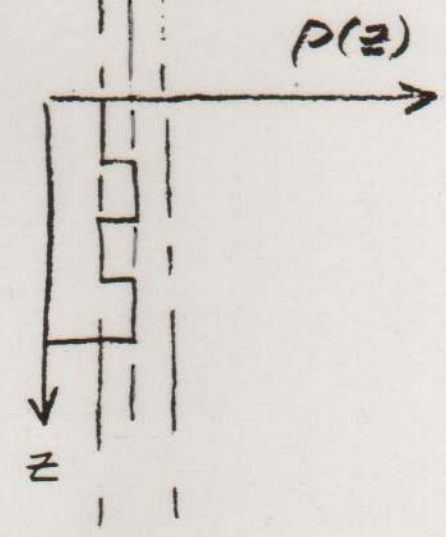
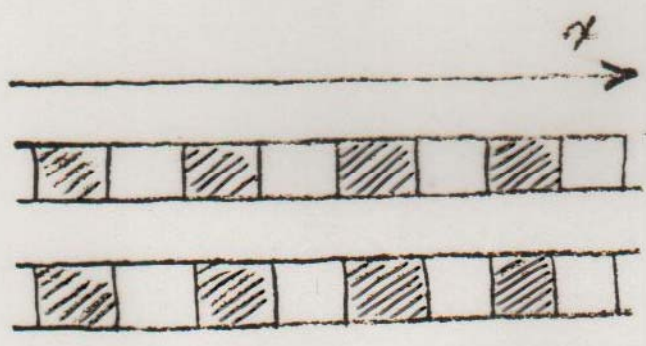
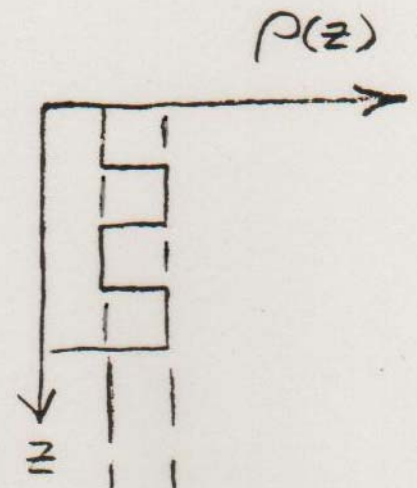
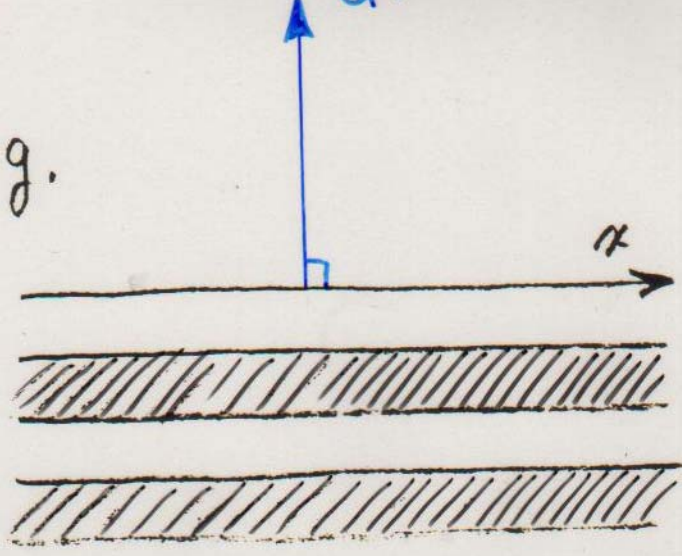
WHERE

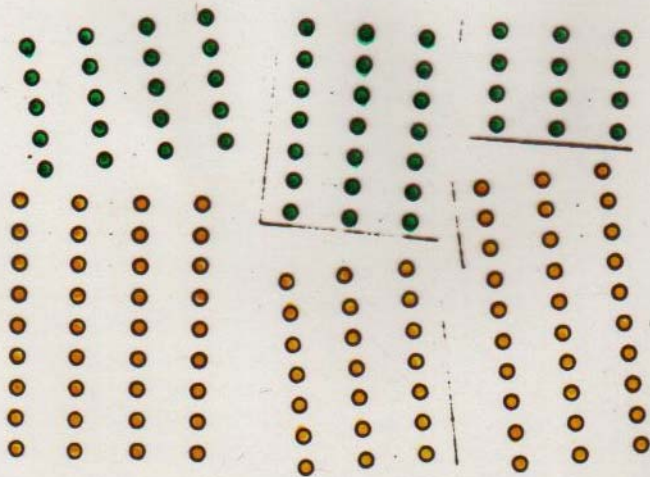
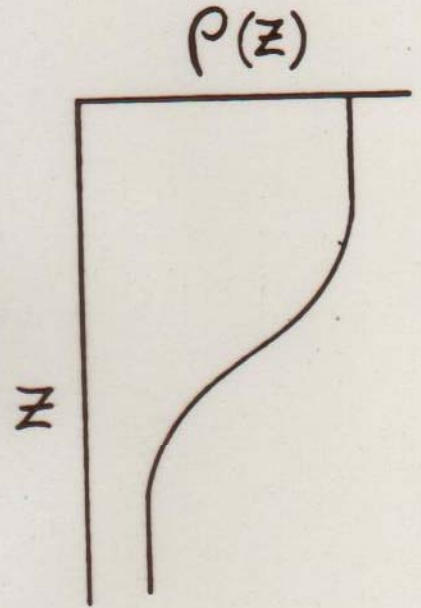
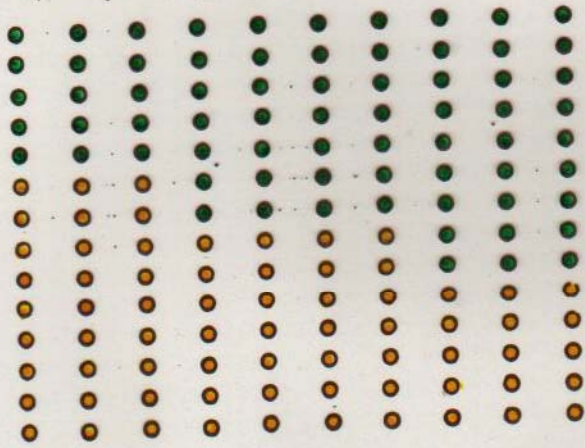
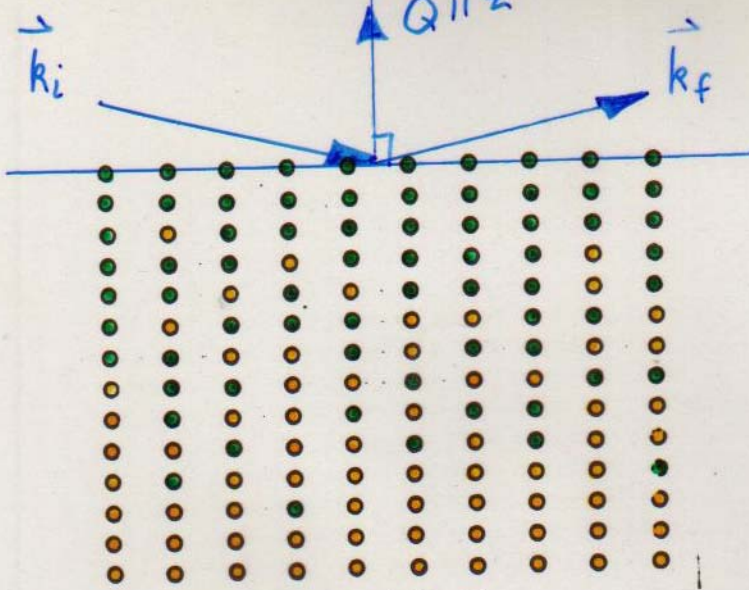
$$\langle \rho(x, y, z) \rangle_{x, y} = \frac{1}{A} \iint_{-\infty}^{+\infty} \rho(x, y, z) dx dy = \bar{\rho}(z) \text{ ONLY}$$

& A = NORMALIZING AREA OF
 THE (x, y) - PLANE

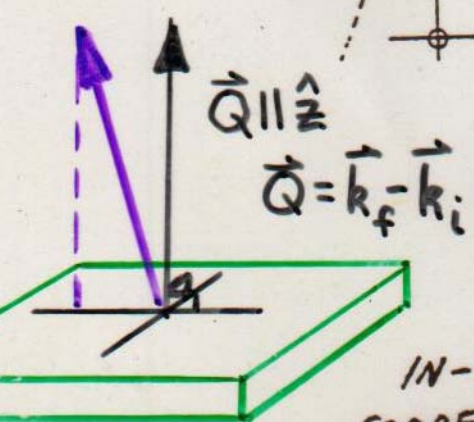
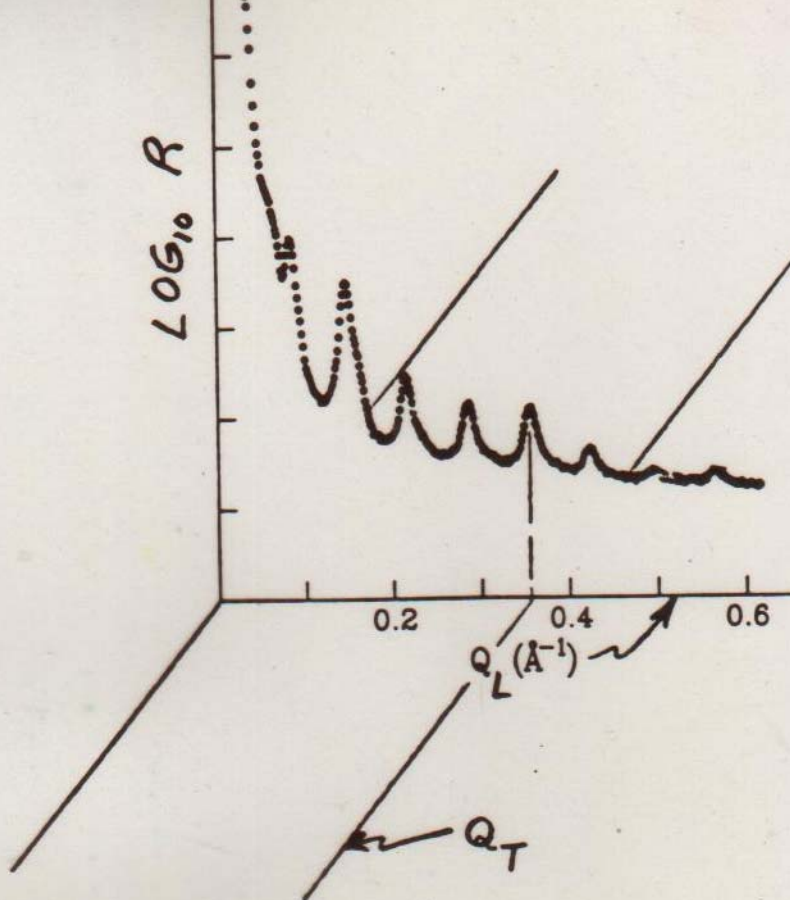
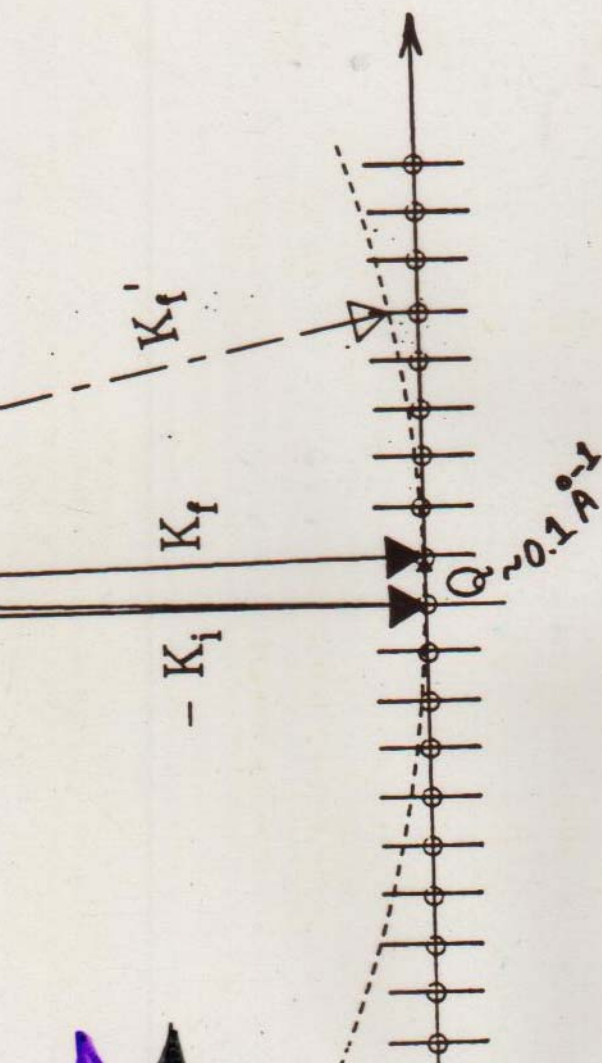
e.g.

$Q(z)$





POSSIBLE MICROSTRUCTURES
CORRESPONDING TO INTERFACIAL
ROUGHNESS



IN-PLANE CORRELATION (?)

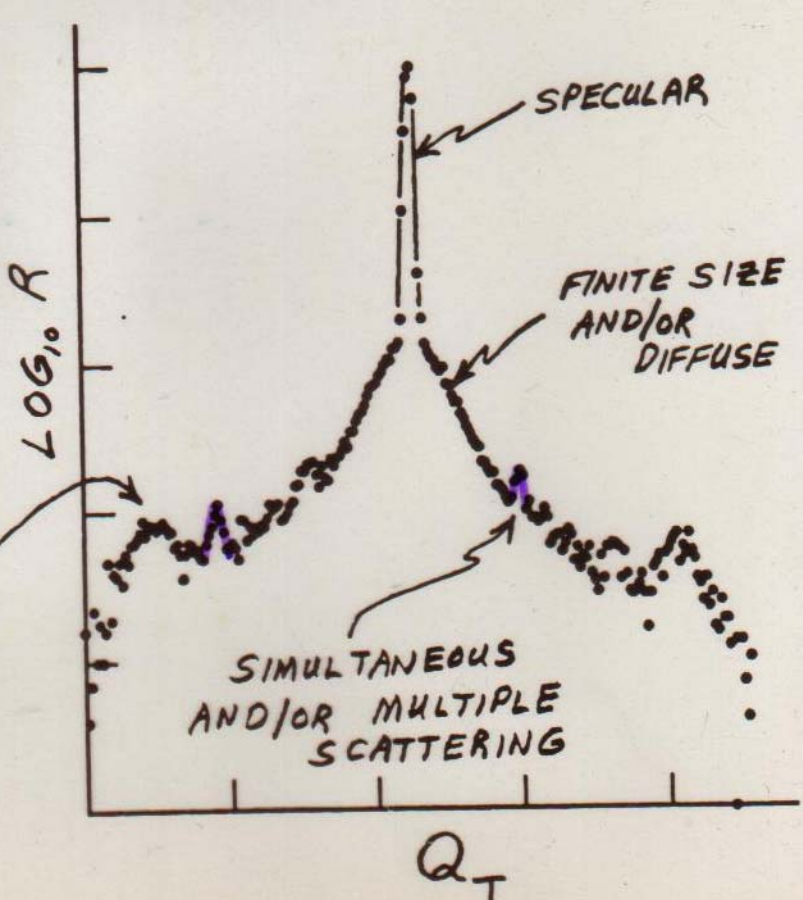
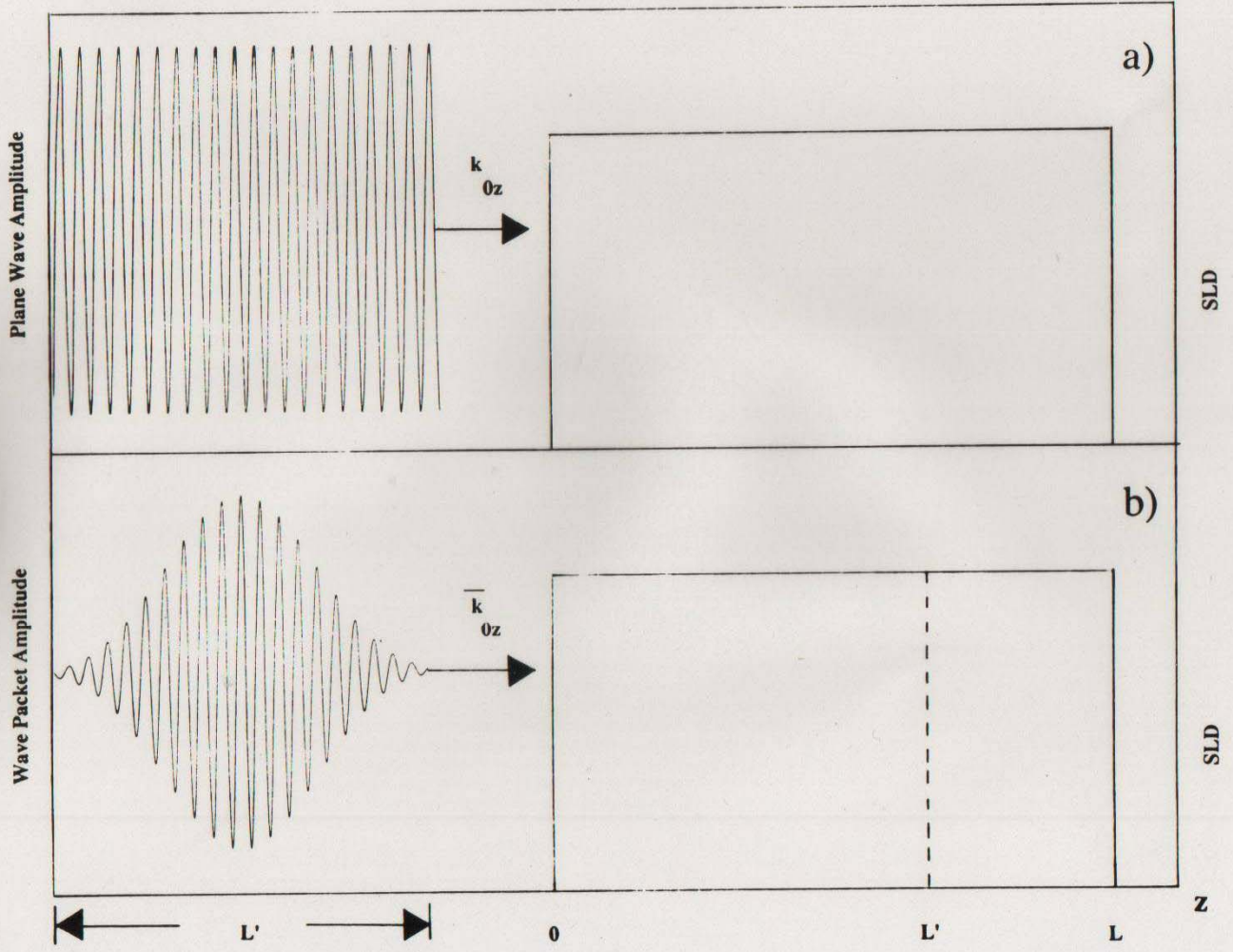


Figure 10



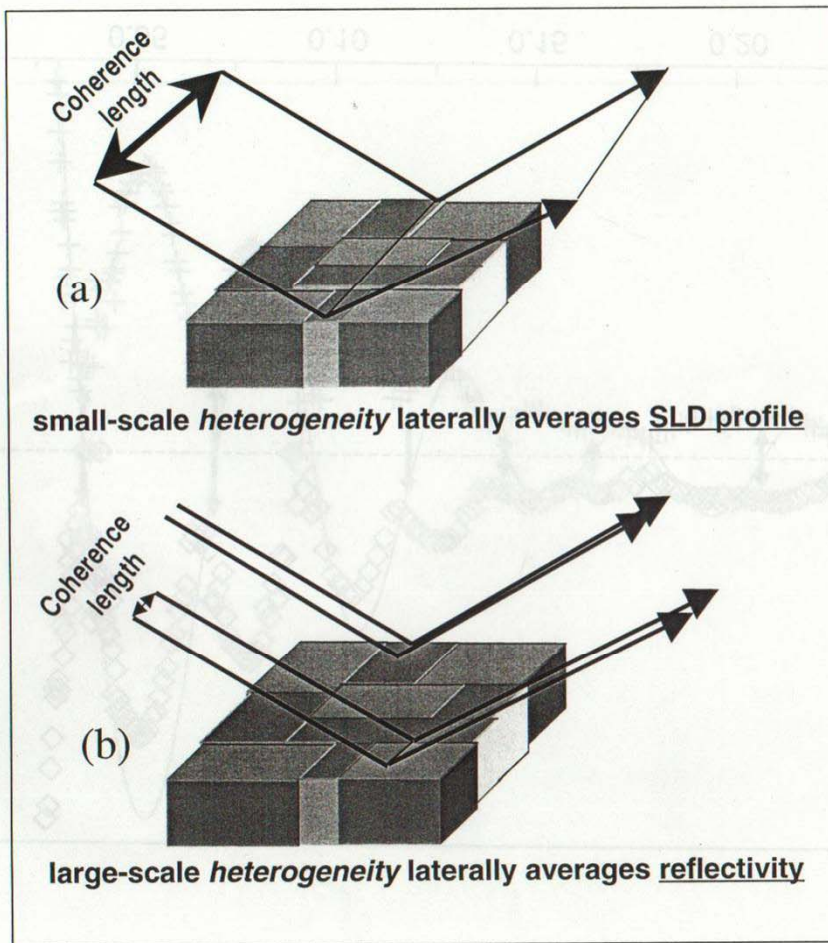
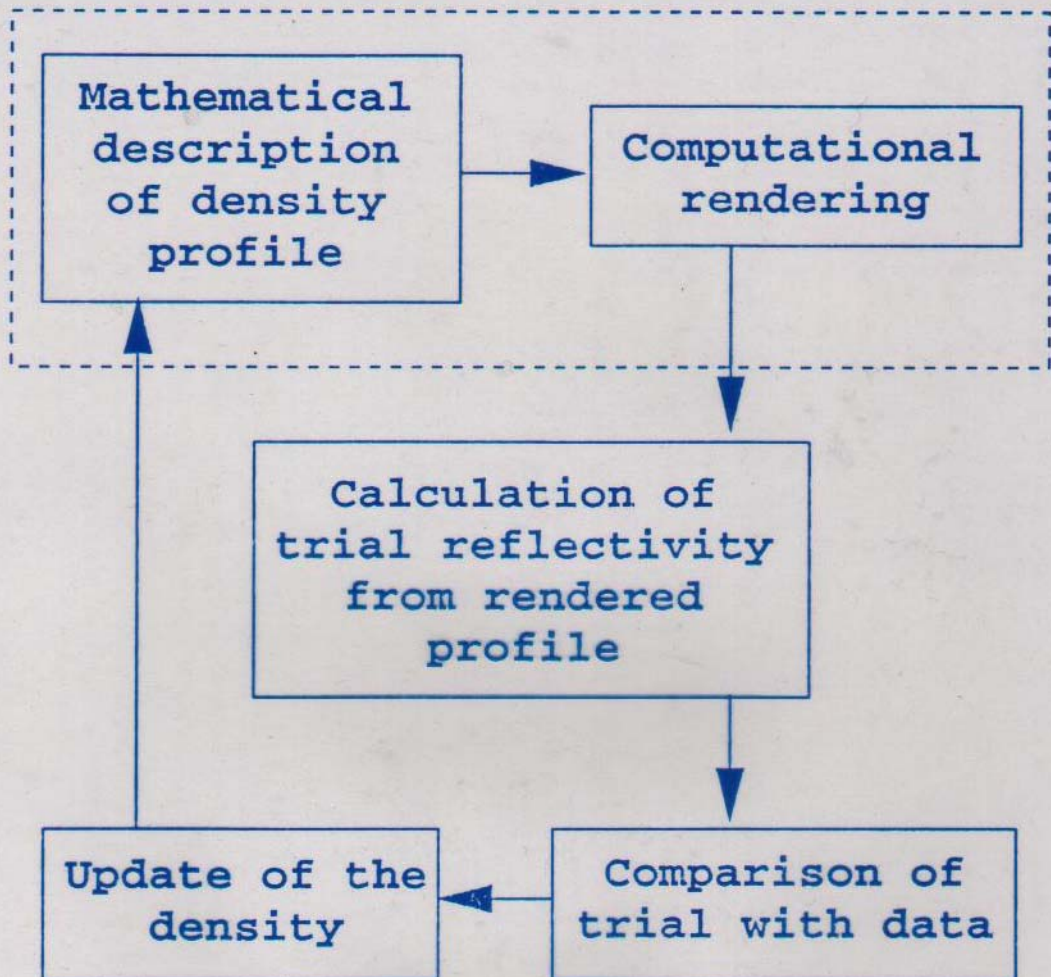


Figure 7.

- SINCE ONLY $|\Psi|^2$ IS A MEASURABLE QUANTITY, CANNOT DIRECTLY OBTAIN REFLECTION AMPLITUDE r , BUT ONLY THE REFLECTIVITY $|r|^2$: $r = |r|e^{i\phi}$: $|r|^2 = |r|e^{-i\phi}|r|e^{+i\phi}$

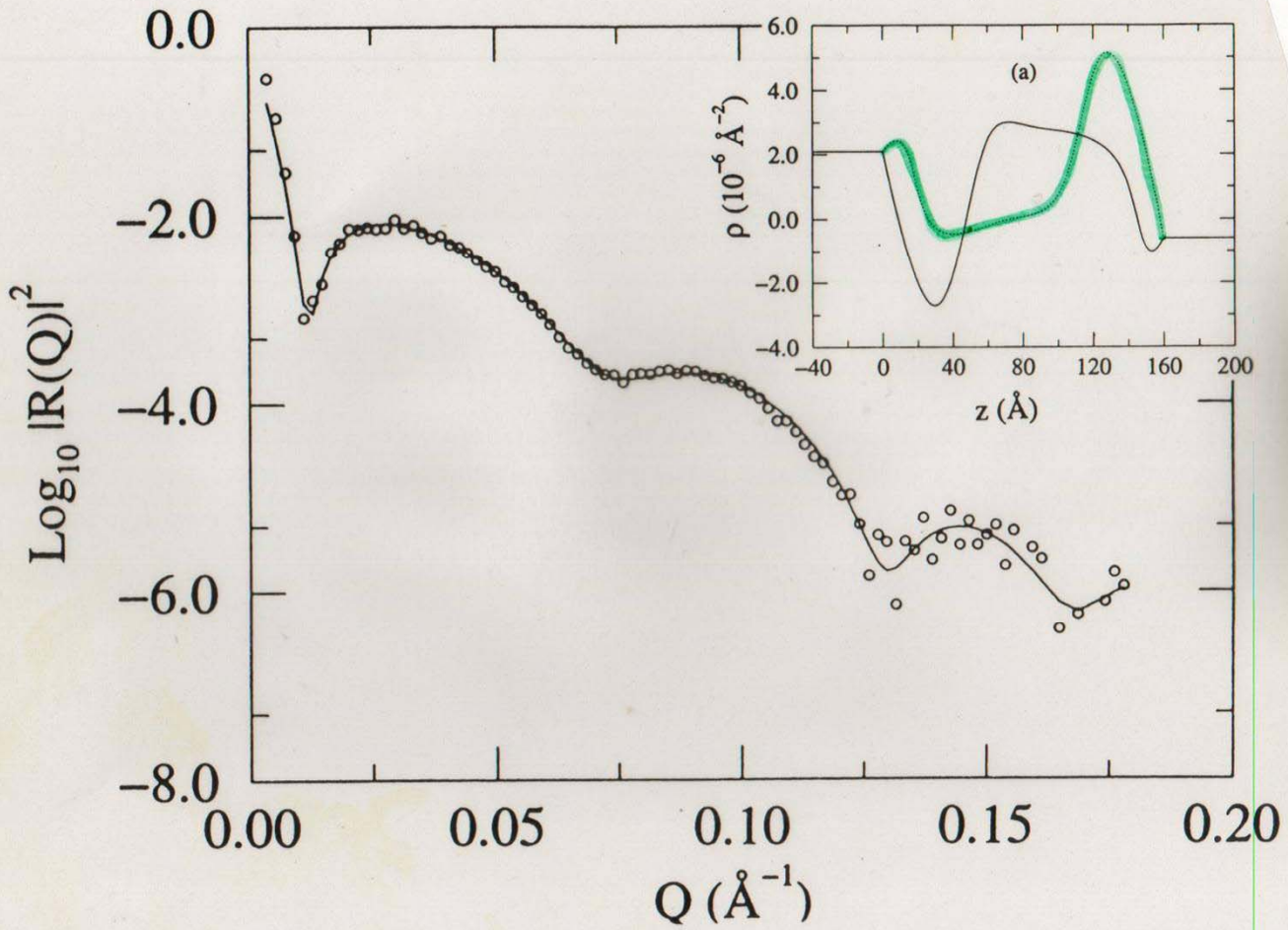
$$|r|^2 = \frac{\text{REFLECTED INTENSITY}}{\text{INCIDENT INTENSITY}}$$

⇒ HENCE, TO OBTAIN $\rho(z)$ FROM $|r(Q)|^2$ REQUIRES A CURVE FITTING ANALYSIS



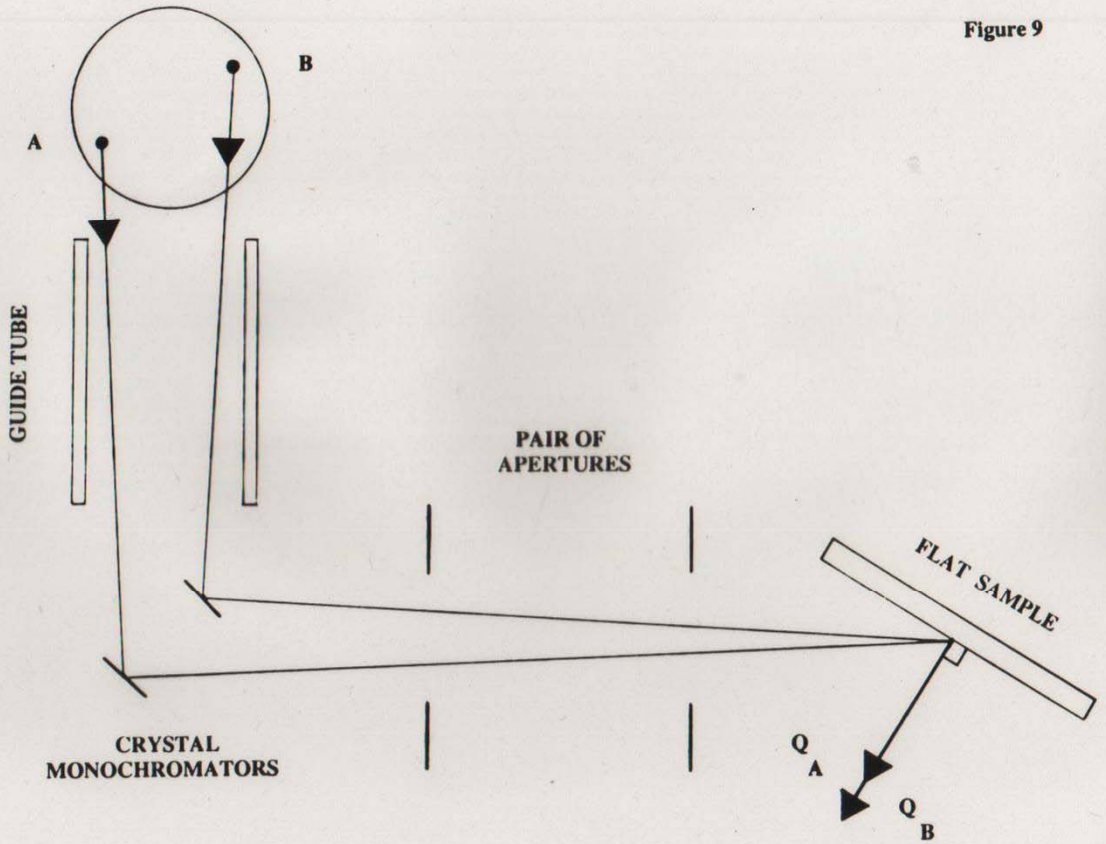
- BOTH MODEL-DEPENDENT & MODEL-INDEPENDENT FITTING METHODS CAN BE USED

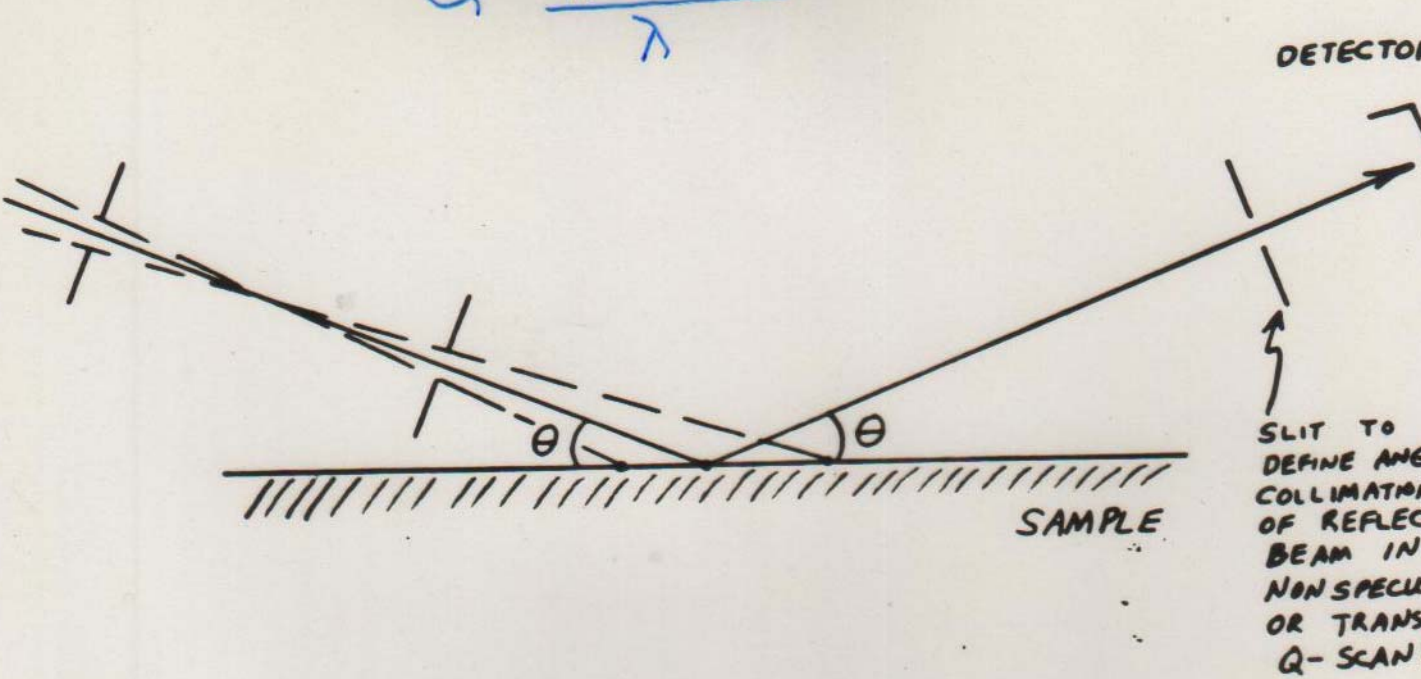
(FIGURE AFTER BERK & MATKREAK)



**EXTENDED LIQUID
HYDROGEN COLD SOURCE**

Figure 9





$$\Delta Q_{\text{LONGITUDINAL}} \approx \frac{\Delta \lambda}{\lambda} Q + \sqrt{\left(\frac{4\pi}{\lambda}\right)^2 - Q^2} \Delta \theta$$

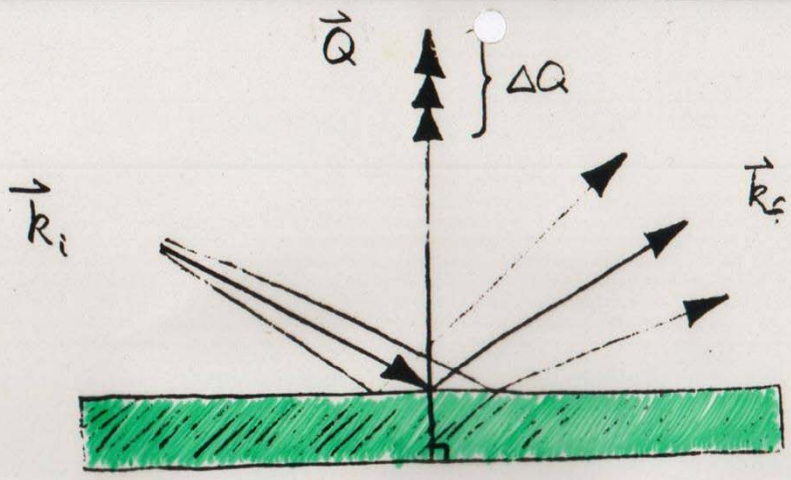
TYPICAL VALUES

$$\left\{ \begin{array}{l} \frac{\Delta \lambda}{\lambda} \approx 0.01 \\ \Delta \theta \approx 1 \text{ min of arc} \end{array} \right.$$

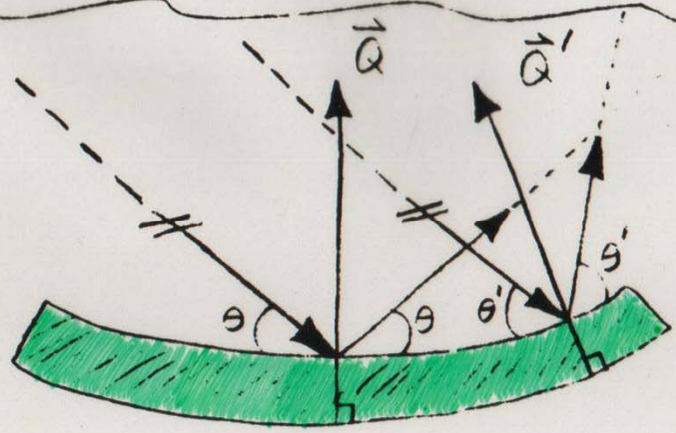
KEEP $\frac{\Delta Q}{Q} \approx \text{CONSTANT}$

$$R_{\text{OBS.}}(Q_0) \approx \left(\frac{0.9394}{\Gamma}\right) \int_{-\Gamma}^{+\Gamma} R_{\text{ACT.}}(Q) e^{-\left(\frac{2.7725}{\Gamma^2}\right)(Q-Q_0)^2} dQ$$

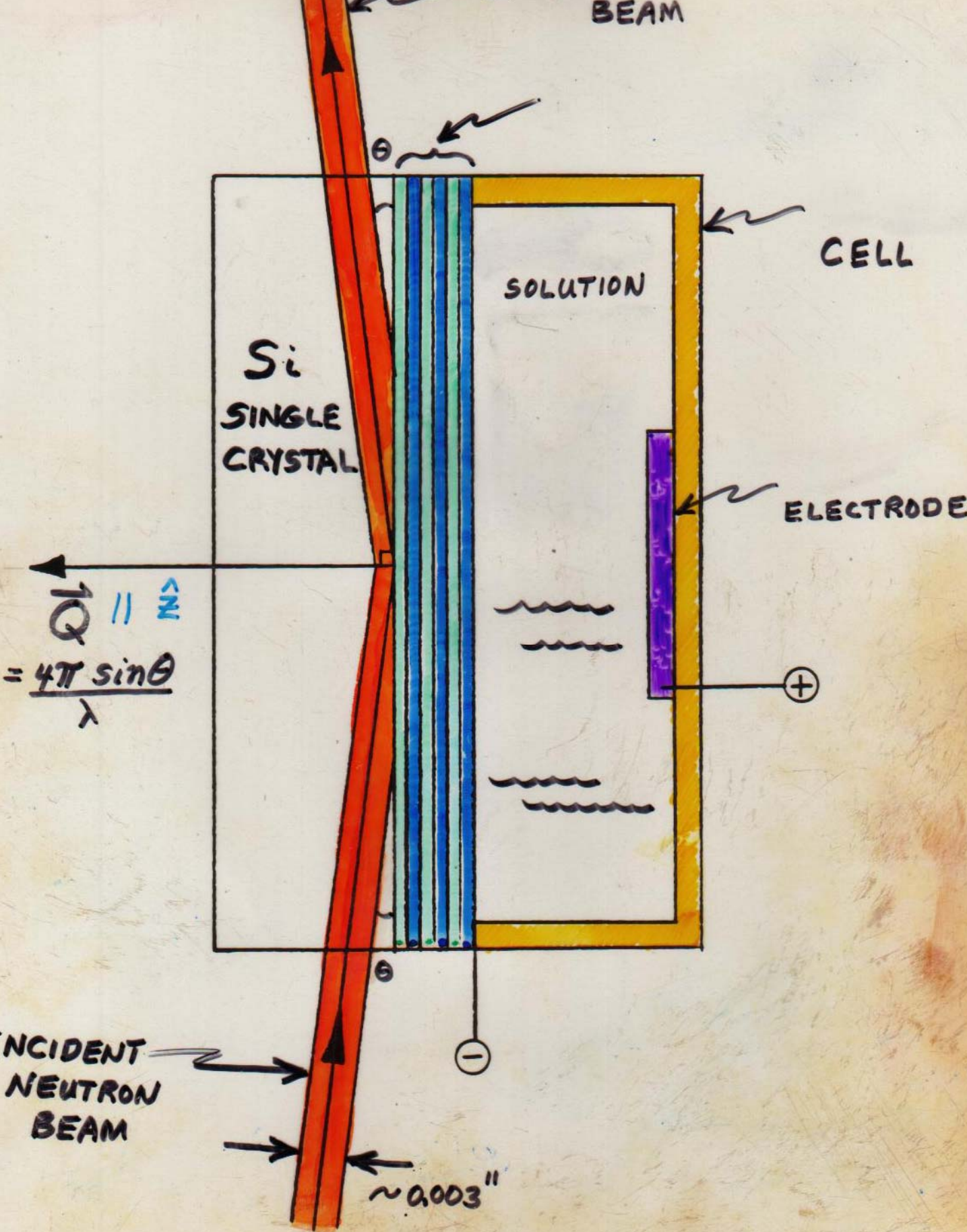
(ASSUMING A GAUSSIAN DISTRIBUTION OF Q-VA)



FLAT
SUBSTRATE



CURVED
SUBSTRATE

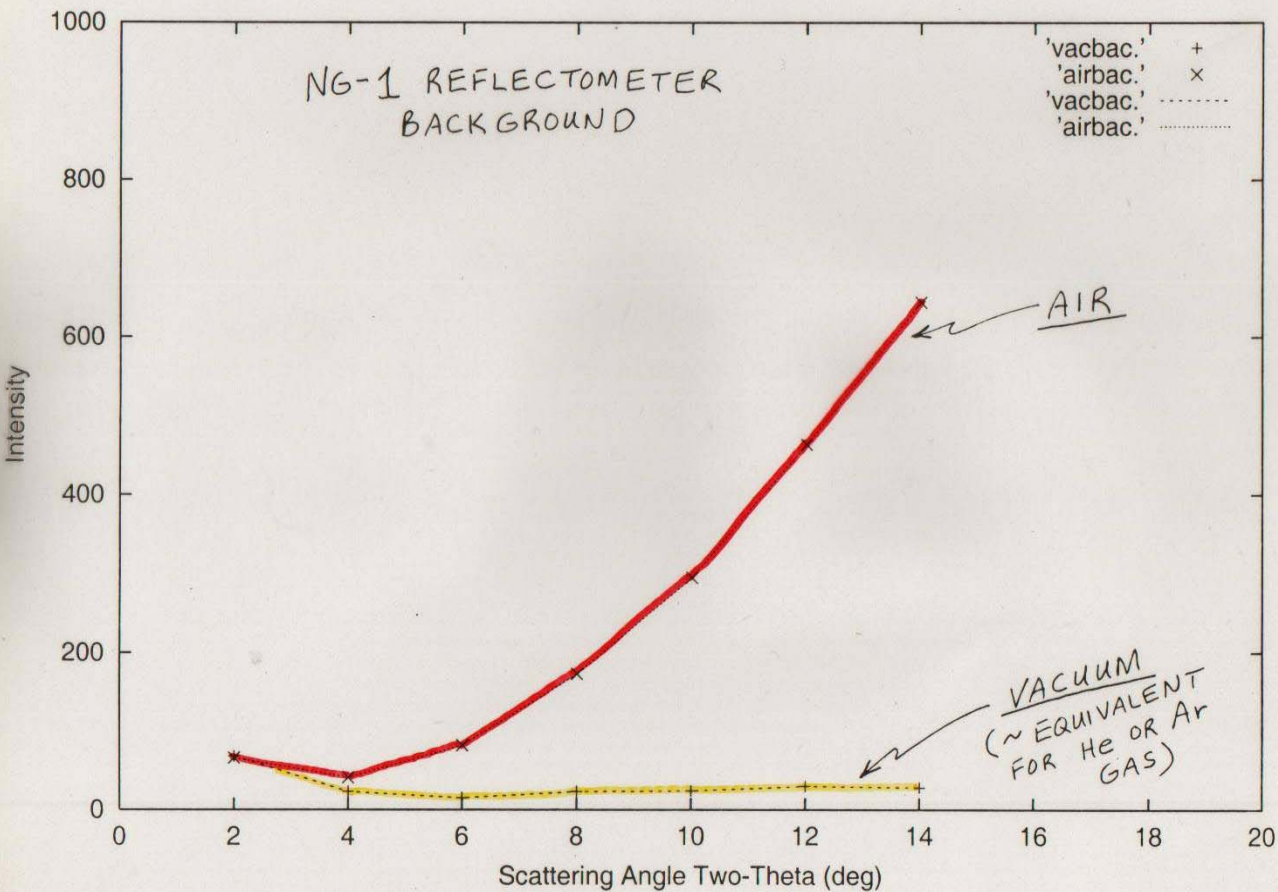


6/2/00

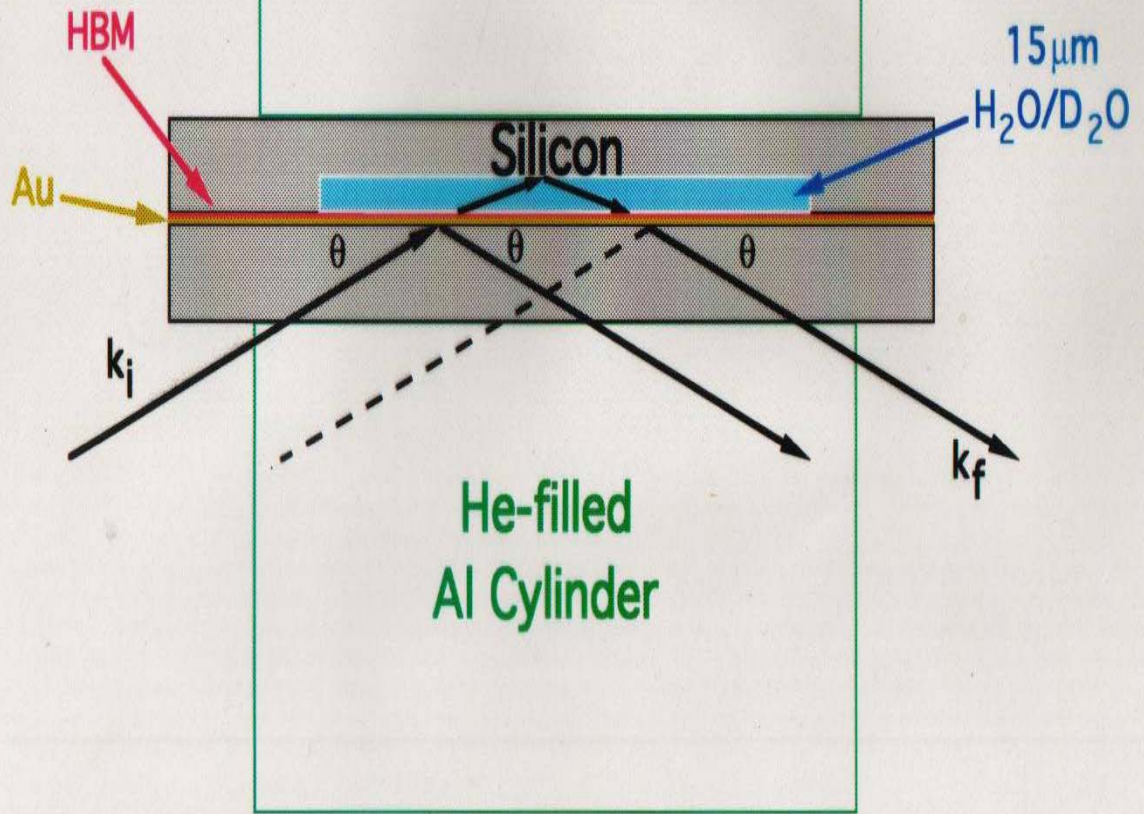
NG-1, NCNR, NIST

NG-1 REFLECTOMETER
BACKGROUND

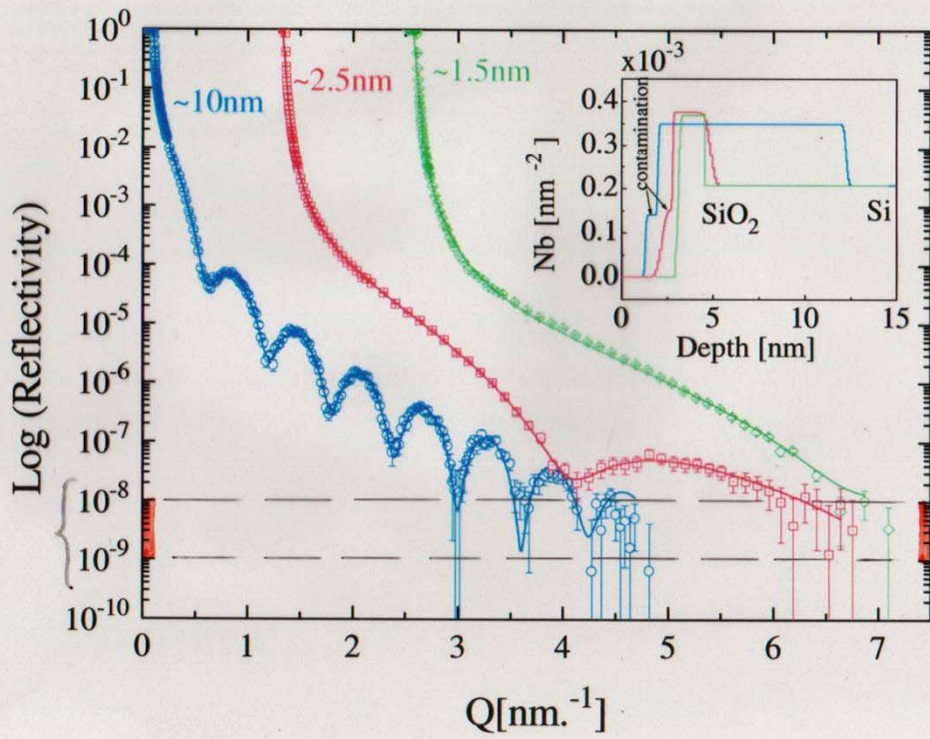
'vacbac.' +
'airbac.' x
'vacbac.'
'airbac.'



Z

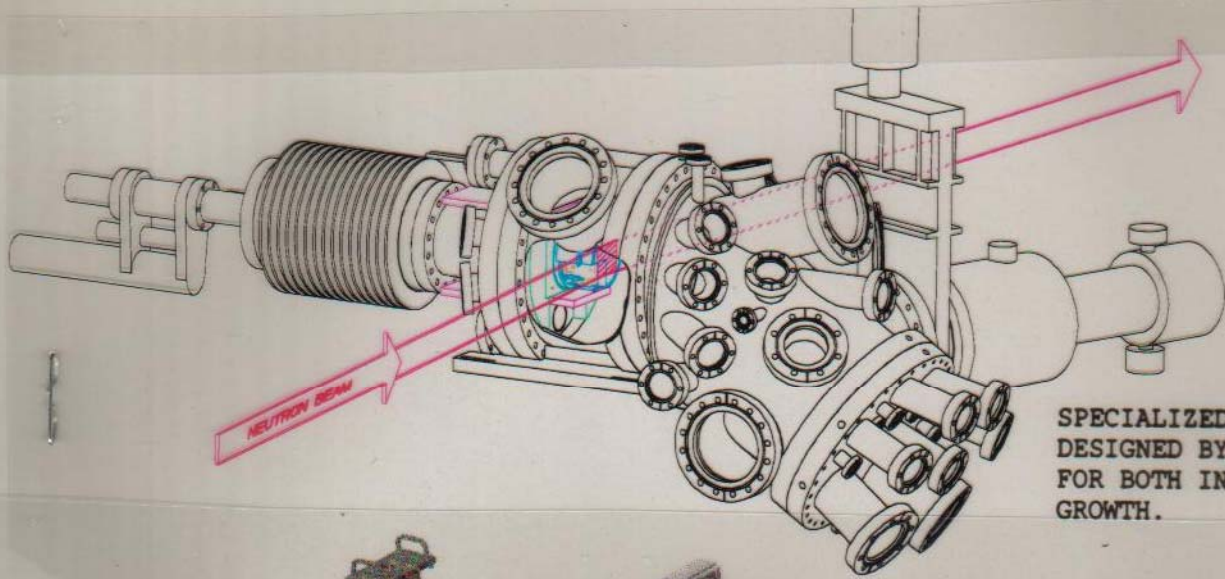
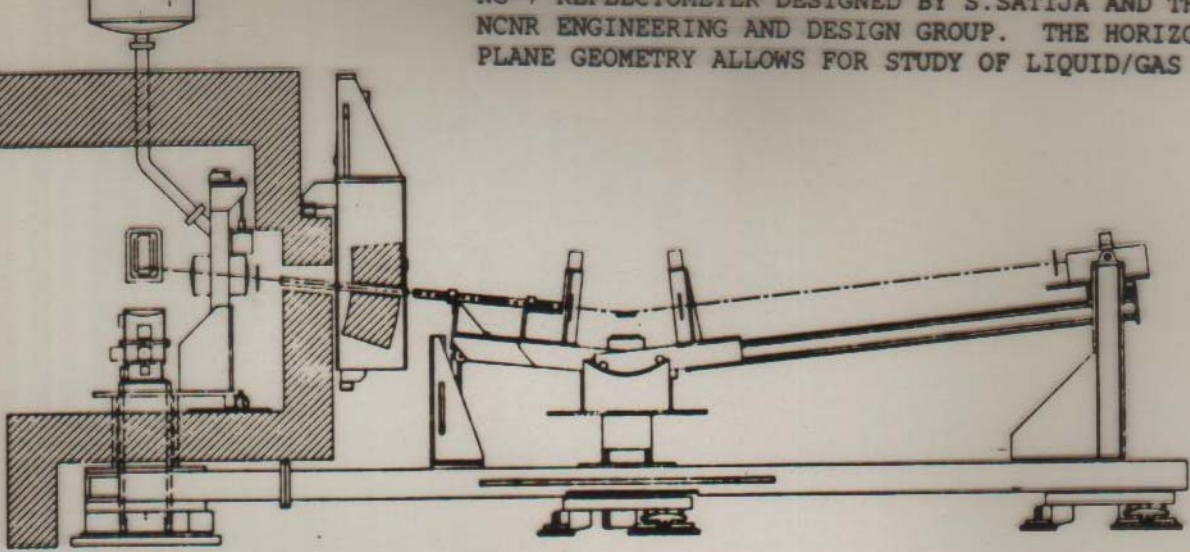


S.KRUEGER et al.

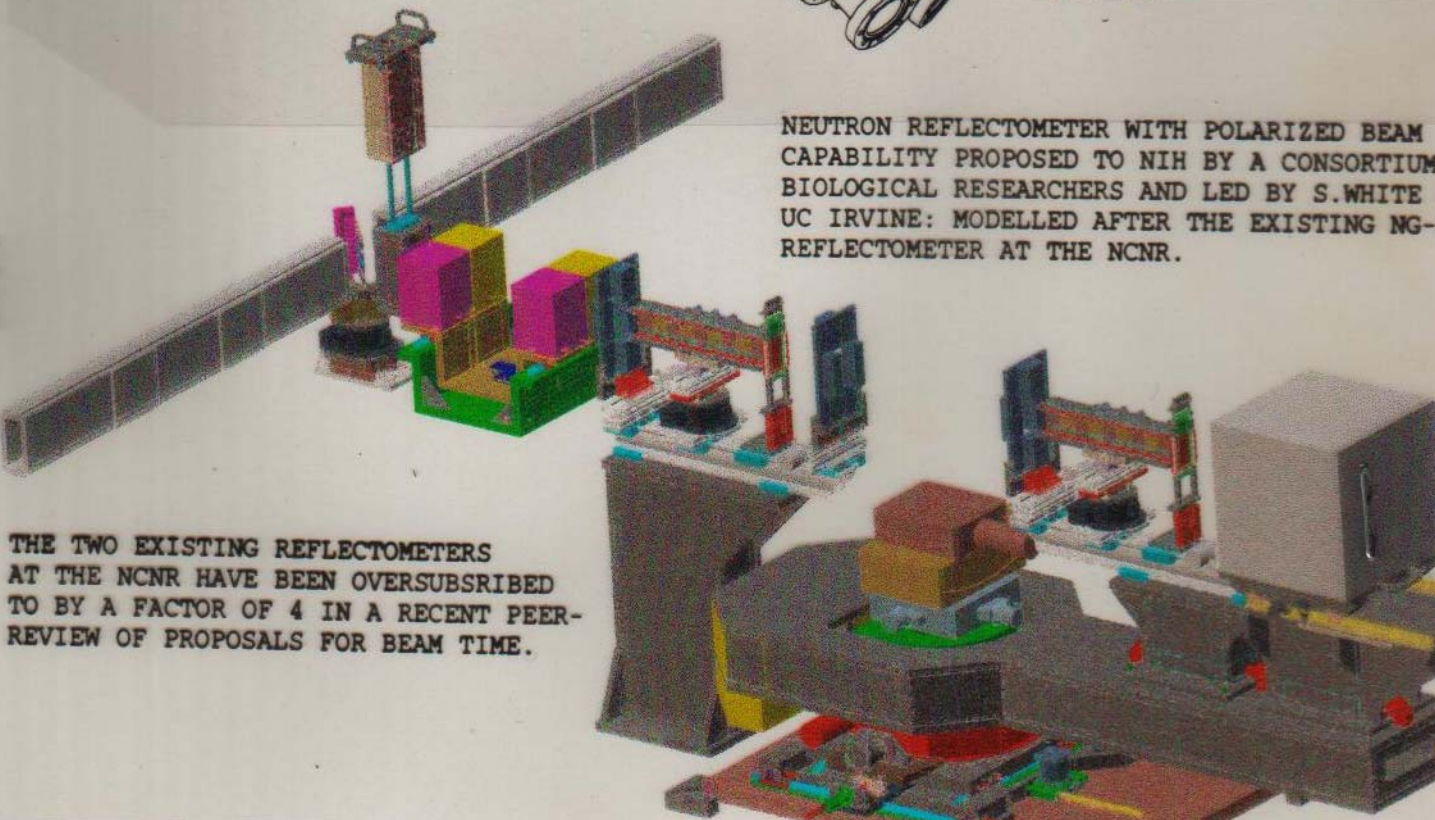


J. DURA et al.

NCNR REFLECTOMETER DESIGNED BY S. SATIJA AND THE EXCELLENCE IN
NCNR ENGINEERING AND DESIGN GROUP. THE HORIZONTAL SAMPLE
PLANE GEOMETRY ALLOWS FOR STUDY OF LIQUID/GAS INTERFACE



SPECIALIZED UHV/MBE CHAMBER
DESIGNED BY J. DURA ET AL
FOR BOTH IN- & EX-SITU FILM
GROWTH.



NEUTRON REFLECTOMETER WITH POLARIZED BEAM
CAPABILITY PROPOSED TO NIH BY A CONSORTIUM
BIOLOGICAL RESEARCHERS AND LED BY S. WHITE
UC IRVINE: MODELLED AFTER THE EXISTING NG-
REFLECTOMETER AT THE NCNR.

THE TWO EXISTING REFLECTOMETERS
AT THE NCNR HAVE BEEN OVERSUBSCRIBED
TO BY A FACTOR OF 4 IN A RECENT PEER-
REVIEW OF PROPOSALS FOR BEAM TIME.

REFERENCES

- * Optics, 3rd Ed., by E.Hecht, Addison Wesley, 1998.
- * Neutron Optics, by V.F.Sears, Oxford University Press, 1989.
- * Principles of Optics, 6th Ed., by M.Born and E.Wolf, Pergamon Press, 1987.
- * Quantum Mechanics, 2nd Ed., by E.Merzbacher, Wiley, 1970.
- * Magnetic Multilayers, Ed. by L.H.Bennett and R.E.Watson; article on "Neutron and X-Ray Diffraction Studies of Magnetic Multilayers" by C.F.Majkrzak, J.F.Ankner, N.F.Berk, and D.Gibbs, World Scientific, 1994, p.299 (contains introductory material on neutron and x-ray reflectometry not specific to magnetic materials alone)
- * Neutron Reflectometry Studies of Thin Films and Multilayered Materials, C.F.Majkrzak, Acta Physica Polonica A 96, 81(1999) -- this article can also be found at the website: <http://www.ncnr.nist.gov> -- along with some additional information on analysing neutron reflectivity data (click on "Summer School Course Materials")

- PHASE-SENSITIVE NEUTRON REFLECTOMETRY, C.F.MAJKRZAK, N.F.BERK, AND U.A.PEREZ-SALAS, LANGMUIR 19, 7796 (2003).
- PHASE SENSITIVE REFLECTOMETRY AND THE UNAMBIGUOUS DETERMINATION OF SCATTERING LENGTH DENSITY PROFILES, C.F.MAJKRZAK AND N.F.BERK, PHYSICA B 336, 27(2003).
- [WWW.NCNR.NIST.GOV](http://www.ncnr.nist.gov) — SEE ANNUAL REPORTS AND SUMMER SCHOOL COURSE MATERIALS
- POLARIZED NEUTRON REFLECTOMETRY, C.F.MAJKRZAK, K.V.O'DONOVAN AND N.F.BERK
- STRUCTURAL INVESTIGATIONS OF MEMBRANES OF INTEREST IN BIOLOGY BY NEUTRON REFLECTOMETRY, C.F.MAJKRZAK, N.F.BERK, S.KRUEGER AND U.PEREZ-SALAS